LiDAR Remote Sensing Data Collection:

Department of Geology & Mineral Industries
Oregon Department of Forestry
Puget Sound LiDAR Consortium

Submitted to:

Puget Sound Regional Council
1011 Western Avenue, Suite 500
Seattle, Washington 98104-1035

Phyllis A. Mann
Kitsap County
911 Carver Street
Bremerton, Washington 98312

Ian Madin, Chief Scientist
Oregon Department of Geology &
Mineral Industries
800 NE Oregon St. Suite 965
Portland OR 97232
(971) 673-1542

Emmor Nile, GISP
GIS Coordinator
Oregon Department of Forestry
2600 State Street, Building E
Salem, Oregon 97310
(503) 945-7418

Submitted by:

Watershed Sciences
215 SE Ninth Avenue, Suite 106
Portland, Oregon 97214
(971) 223-5152

February 19, 2008

LiDAR Remote Sensing Data Collection:
DoGAMI, ODF Study Areas

TABLE OF CONTENTS

Prepared by **Watershed Sciences**

1. Overview

1.1 DoGAMI and ODF Study Areas

Watershed Sciences, Inc. (WS) collected Light Detection and Ranging (LiDAR) data for the Department of Geology and Mineral Industries (DoGAMI) and the Oregon Department of Forestry (ODF) March 15 - May 9, and September 29 – October 8, 2007. The Areas of Interest (AOIs) cover portions of eight counties in northwest Oregon. The extent of requested LiDAR area totals ~1,491,495 acres; the map below shows the extent of the LiDAR area to be delivered, covering ~1,517,599 acres. The delivered acreage for the study area is greater than the original amount due to buffering of the original AOIs and flight planning optimization.

Figure 1. Extent of Department of Geology and Mineral Industries (DoGAMI) and Oregon Department of Forestry (ODF) Areas of Interest (AOIs):
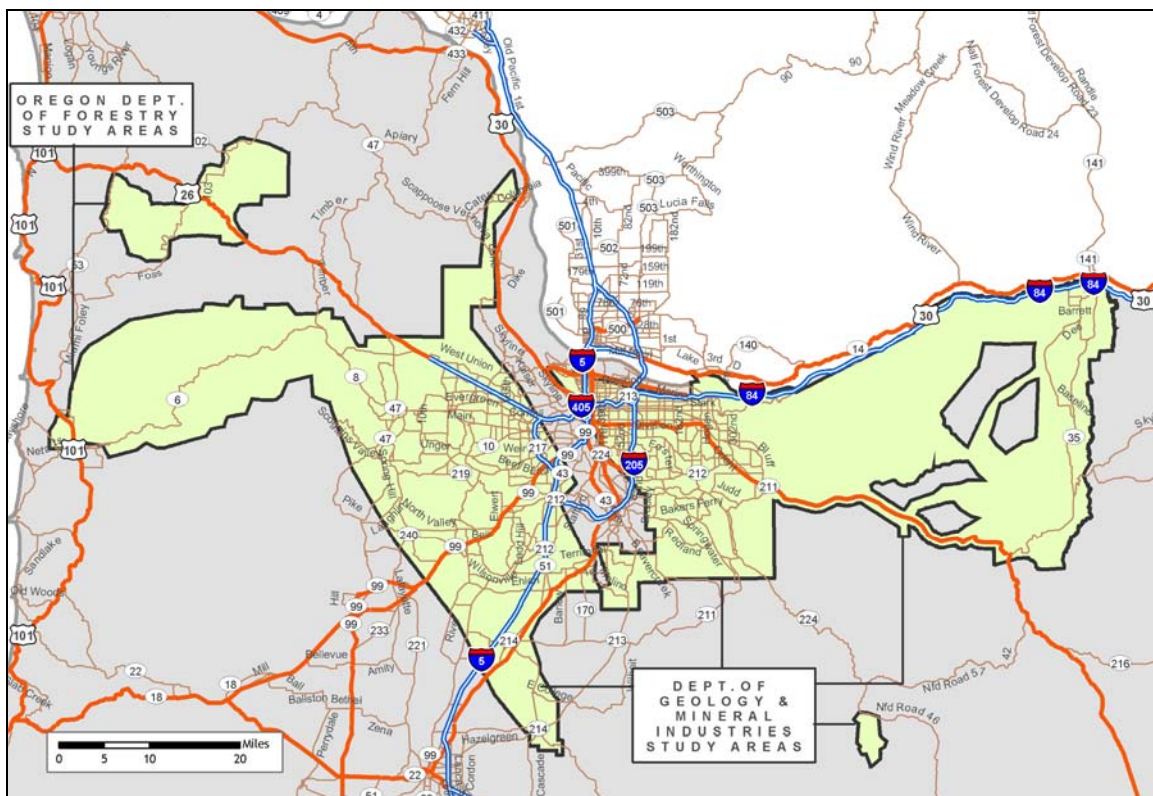
Portions of the following seven 7.5' USGS quads are included in this delivery:

7.5' USGS QUAD NAME	7.5' USGS QUAD NUMBER
Bedford Point	45122B2
Elwood	45122B3
Colton	45122B4
Estacada	45122C3
Redland	45122C4
Damascus	45122D4
Camas	45122E4

The location and extent of these quads is shown in Figure 2 below, and covers 116,655 acres. The total delivered acreage to date is detailed below.

ODF AOIs	
Delivery Date	**Acres**
September 13, 2007	85,229
December 3, 2007	94,523
December 18, 2007	132,300
Portland AOI	
Delivery Date	**Acres**
October 15, 2007	209,903
November 1, 2007	118,909
November 12, 2007	167,191
January 29, 2008	83,577
February 19, 2008	116,655
Total	*1,008,287*

Figure 2. 7.5' USGS Quads provided in this delivery.
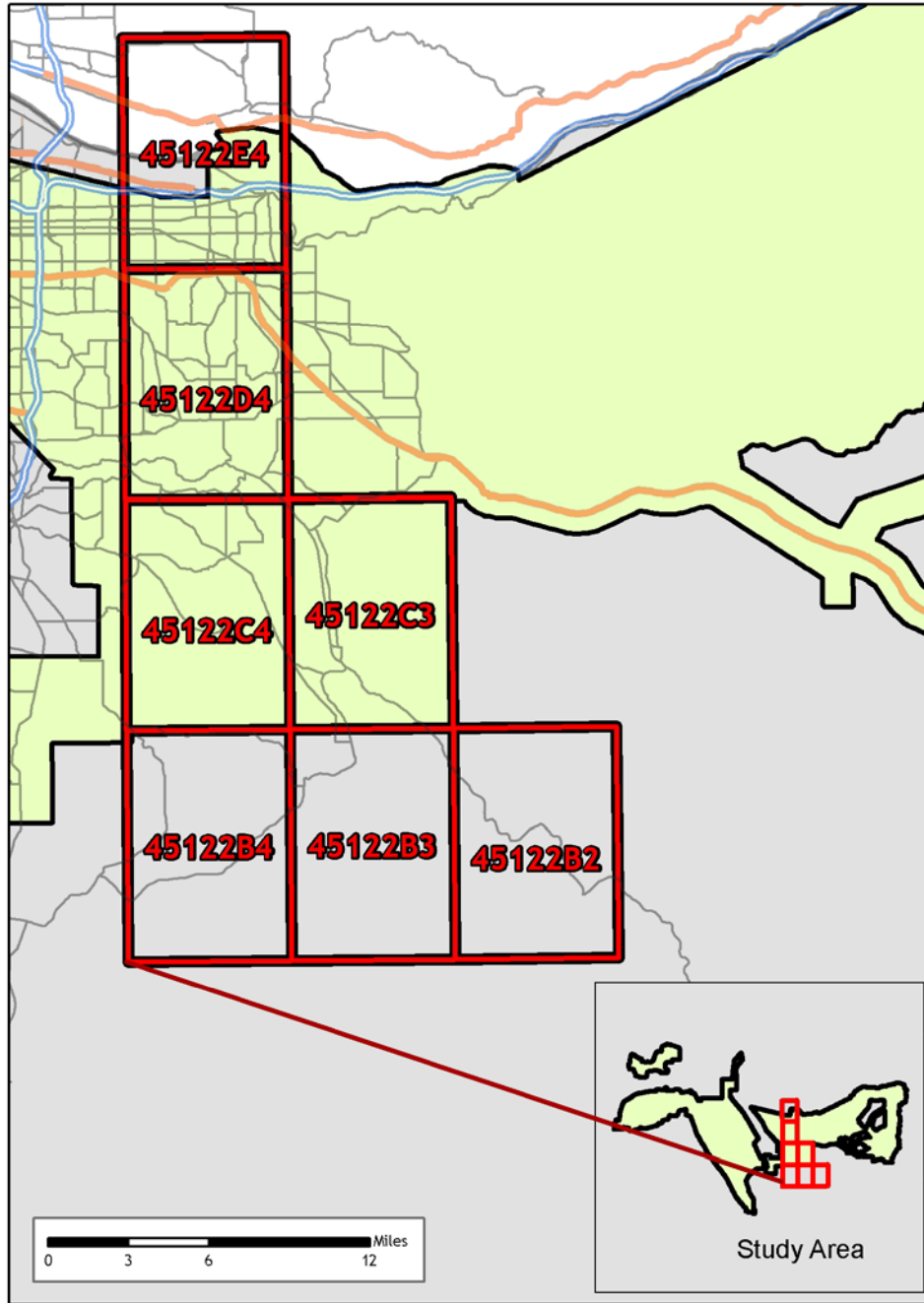
1.2 Accuracy and Resolution

Laser points were collected over the study areas using a LiDAR laser system set to acquire points with full overlap (i.e., ≥50% side-lap) to ensure complete coverage and minimize laser shadows created by buildings and tree canopies. **Figure 3** below illustrates the location, swath width and the overlap of the planned flight lines for the DOGAMI & ODF study areas. Real-time kinematic (RTK) surveys were conducted in multiple locations throughout the study area for quality assurance purposes. The accuracy of the LiDAR data is described as standard deviations of divergence (sigma ~ σ) from RTK ground survey points and root mean square error (RMSE) which considers bias (upward or downward). These statistics are calculated cumulatively. For the DOGAMI / ODF study areas, the data have the following accuracy statistics:

- RMSE of 0.11 feet
- 1-sigma absolute deviation of 0.11 feet
- 2-sigma absolute deviation of 0.23 feet [1]

Data resolution specifications are for ≥8 pts per m^2. Section 4.2 demonstrates that total pulse density for the Portland AOI delivered to date is 6.91 points per m^2 (0.64 points per square foot).

1.3 Data Format, Projection, and Units

Deliverables include point data in *.las v 1.1 and ascii format, 3-foot resolution bare ground model ESRI GRID, 3-foot resolution above ground surface ESRI GRID, 1.5-foot resolution intensity images in GeoTIFF format, Smoothed Best Estimate of Trajectory (5Hz frequency) information in ascii text format, and data report.

- ODF AOIs are delivered in Oregon Lambert, EPSG 2992, with horizontal units in International Feet and vertical units in US Survey Feet, in the NAD83/NAVD88 datum (Geoid 03).

- All other AOIs are delivered in Oregon State Plane North, with horizontal units in International Feet and vertical units in US Survey Feet, in the NAD83 HARN/NAVD88 datum (Geoid 03).

---

[1] Accuracy assessment based on comparison of RTK survey points to LiDAR points collected in the same acquisition but in a more easily accessible study area.

2. Acquisition

2.1 Airborne Survey – Instrumentation and Methods

The LiDAR survey utilized a Leica ALS50 Phase II mounted in Cessna Caravan 208B and an Optech 3100 laser system mounted in a Cessna Caravan 208. The full survey was conducted March 15 - May 9, and September 29 – October 8, 2007.

The Leica ALS50 Phase II system was set to acquire ≥105,000 laser pulses per second (i.e. 105 kHz pulse rate) and flown at 900 meters above ground level (AGL), capturing a scan angle of ±14° from nadir[2]. The Optech 3100 system was set to acquire 71,000 laser pulses per second (i.e. 71 kHz pulse rate) and flown at 900 meters above ground level (AGL) capturing a scan angle of ±14° from nadir. These settings are developed to yield points with an average native density of ≥8 points per square meter over terrestrial surfaces. The native pulse density is the number of pulses emitted by the LiDAR system. Some types of surfaces (i.e., dense vegetation or water) may return fewer pulses than the laser originally emitted. Therefore, the delivered density can be less than the native density and lightly variable according to distributions of terrain, land cover and water bodies.

The completed area was surveyed with opposing flight line side-lap of ≥50% (≥100% overlap) to reduce laser shadowing and increase surface laser painting. The system allows up to four range measurements per pulse, and all discernable laser returns were processed for the output dataset.

To solve for laser point position, it is vital to have an accurate description of aircraft position and attitude. Aircraft position is described as x, y and z and measured twice per second (2 Hz) by an onboard differential GPS unit. Aircraft attitude is measured 200 times per second (200 Hz) as pitch, roll and yaw (heading) from an onboard inertial measurement unit (IMU).

Figure 3 below illustrates the location, swath width and overlap of the planned flight lines for the DOGAMI study areas.

---

[2] Nadir refers to the perpendicular vector to the ground directly below the aircraft. Nadir is commonly used to measure the angle from the vector and is referred to a "degrees from nadir".

LiDAR Remote Sensing Data: Department of Geology and Mineral Industries and Oregon Department of Forestry
Prepared by Watershed Sciences, Inc.   *February 19, 2008*

Figure 3. Planned flight lines for the ODF/DOGAMI AOIs illustrated over 3-D GoogleEarth image, showing flightline locations, swath width, and overlap between flight lines.
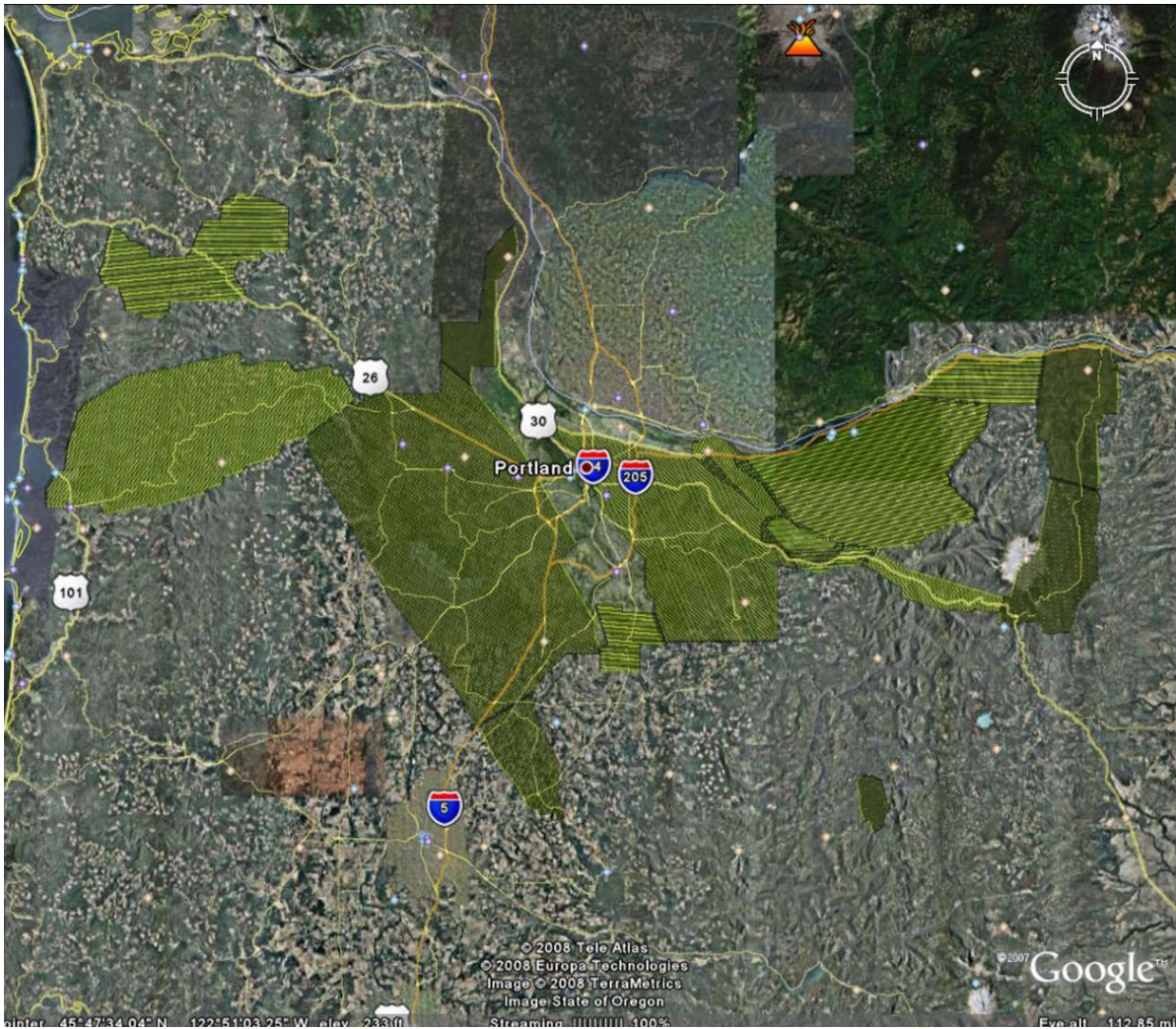
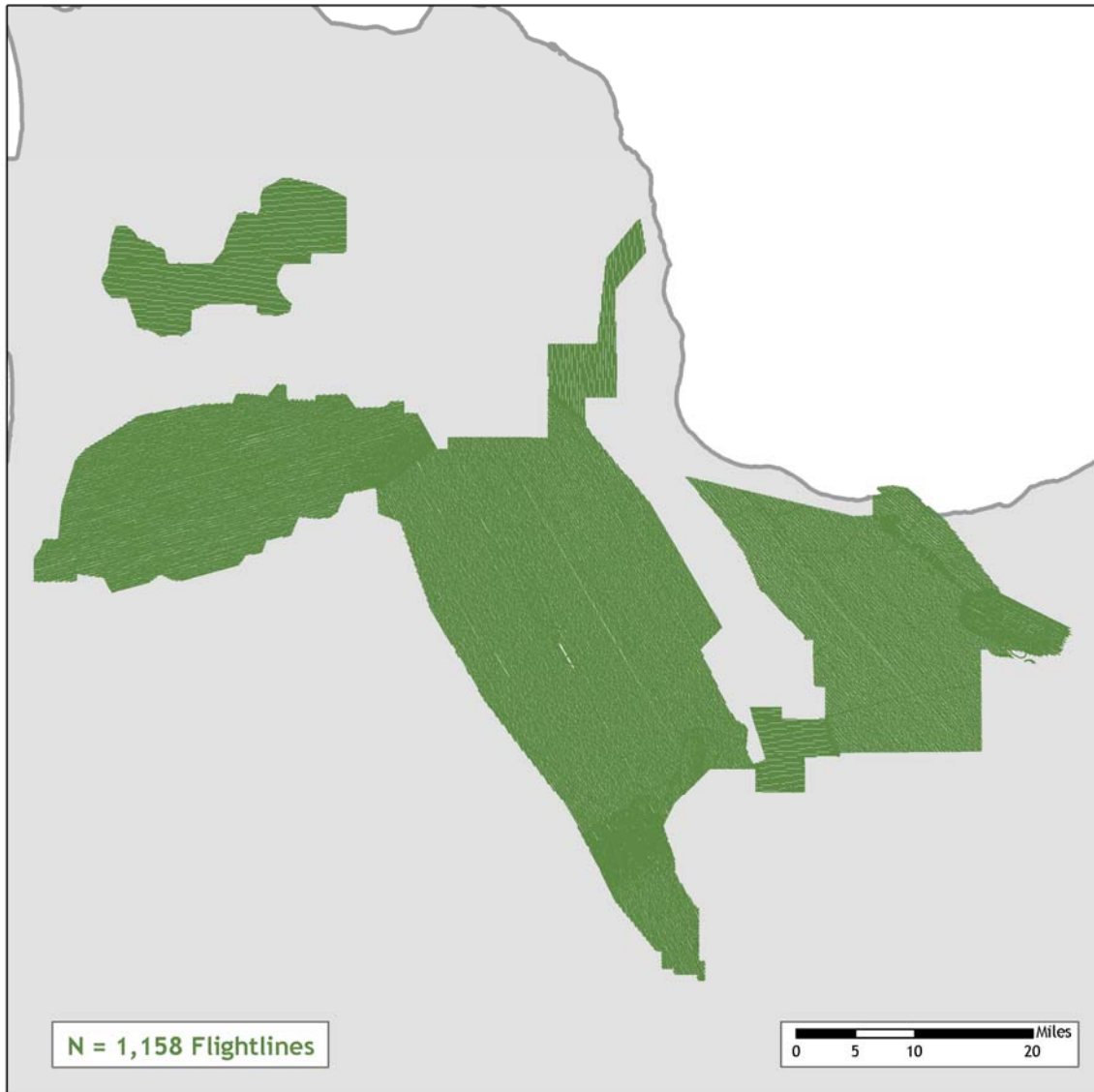**LiDAR Remote Sensing Data: Department of Geology and Mineral Industries and Oregon Department of Forestry**
Prepared by Watershed Sciences, Inc.   *February 19, 2008*

Figure 4. Actual flightlines in ODF and DOGAMI study areas.

N = 1,158 Flightlines

LiDAR Remote Sensing Data: Department of Geology and Mineral Industries and Oregon Department of Forestry
Prepared by Watershed Sciences, Inc. *February 19, 2008*

2.2 Ground Survey – Instrumentation and Methods

During the LiDAR survey of the study area, a static (1 Hz recording frequency) ground survey was conducted over monuments with known coordinates. Coordinates are provided in **Table 1** and shown below in **Figure 5**. After the airborne survey, the static GPS data are processed using triangulation with CORS stations and checked against the Online Positioning User Service (OPUS[3]) to quantify daily variance. Multiple sessions are processed over the same monument to confirm antenna height measurements and reported position accuracy.

Table 1. Base Station Surveyed Coordinates, (NAD83/NAVD88, OPUS corrected) used for kinematic post-processing of the aircraft GPS data for the ODF/DOGAMI AOIs.

| Study Area | Base Station ID | Datum NAD83(HARN) | | GRS80 |
		Latitude (North)	Longitude (West)	Ellipsoid Height (m)
DOGAMI	ORMI_1	45 07 38.77347	122 47 50.69501	29.077
DOGAMI	SCJR_1	45 01 16.71080	122 44 37.15483	77.597
DOGAMI	ORMI_2	45 30 30.86516	123 05 27.70581	26.630
DOGAMI	ORMI_3	45 24 08.24317	122 54 59.88436	32.208
DOGAMI	ORMI_4	45 14 34.58806	122 46 02.63126	37.028
DOGAMI	SCJR3	44 54 08.93624	122 42 08.33058	325.829
DOGAMI	ORJR_1	45 19 53.37805	122 20 55.26176	95.011
DOGAMI	ORJR_2	45 27 24.86103	122 33 33.65264	181.756
DOGAMI	ORJM2	45 27 24.86103	122 33 33.65264	181.756
DOGAMI	ORJR5	45 46 22.21129	122 53 01.10672	3.562
DOGAMI	ORJR6	45 53 43.01413	122 48 48.08575	6.210
DOGAMI	ORSP14	45 52 23.25109	123 33 38.28134	108.139
DOGAMI	ORSP15	45 39 02.12095	123 16 33.08583	136.147
DOGAMI	ORSP16	45 39 02.12095	123 16 33.08583	136.147
DOGAMI	ORJR21	45 18 23.10077	121 49 49.67527	808.484
DOGAMI	ORSP20	45 23 19.99348	122 09 23.35649	359.167
DOGAMI	ORSP22	45 33 29.27716	122 38 34.17056	47.016
DOGAMI	RD4237	45 28 29.30798	122 23 46.92313	118.878
ODF	ORSP10	45 51 45.02398	123 35 01.16219	139.9685
ODF	ORSP11	45 51 16.03468	123 32 26.33048	187.864
ODF	ORSP12	45 37 08.06456	123 23 50.39774	402.8955
ODF	ORSP13	45 29 59.43934	123 38 32.06929	280.969
ODF	ORSP14	45 52 23.25109	123 33 38.28134	108.139

---

[3] Online Positioning User Service (OPUS) is run by the National Geodetic Survey to process corrected monument positions.

Multiple DGPS units are used for the ground real-time kinematic (RTK) portion of the survey. To collect accurate ground surveyed points, a GPS base unit is set up over monuments to broadcast a kinematic correction to a roving GPS unit. The ground crew uses a roving unit to receive radio-relayed kinematic corrected positions from the base unit. This method is referred to as real-time kinematic (RTK) surveying and allows precise location measurement ($\sigma \leq 1.5$ cm ~ 0.6 in). 10,131 RTK ground points were collected throughout the study areas and compared to LiDAR data for accuracy assessment. **Figure 5** shows base station locations and **Figures 6-13** show detailed views of RTK point locations.

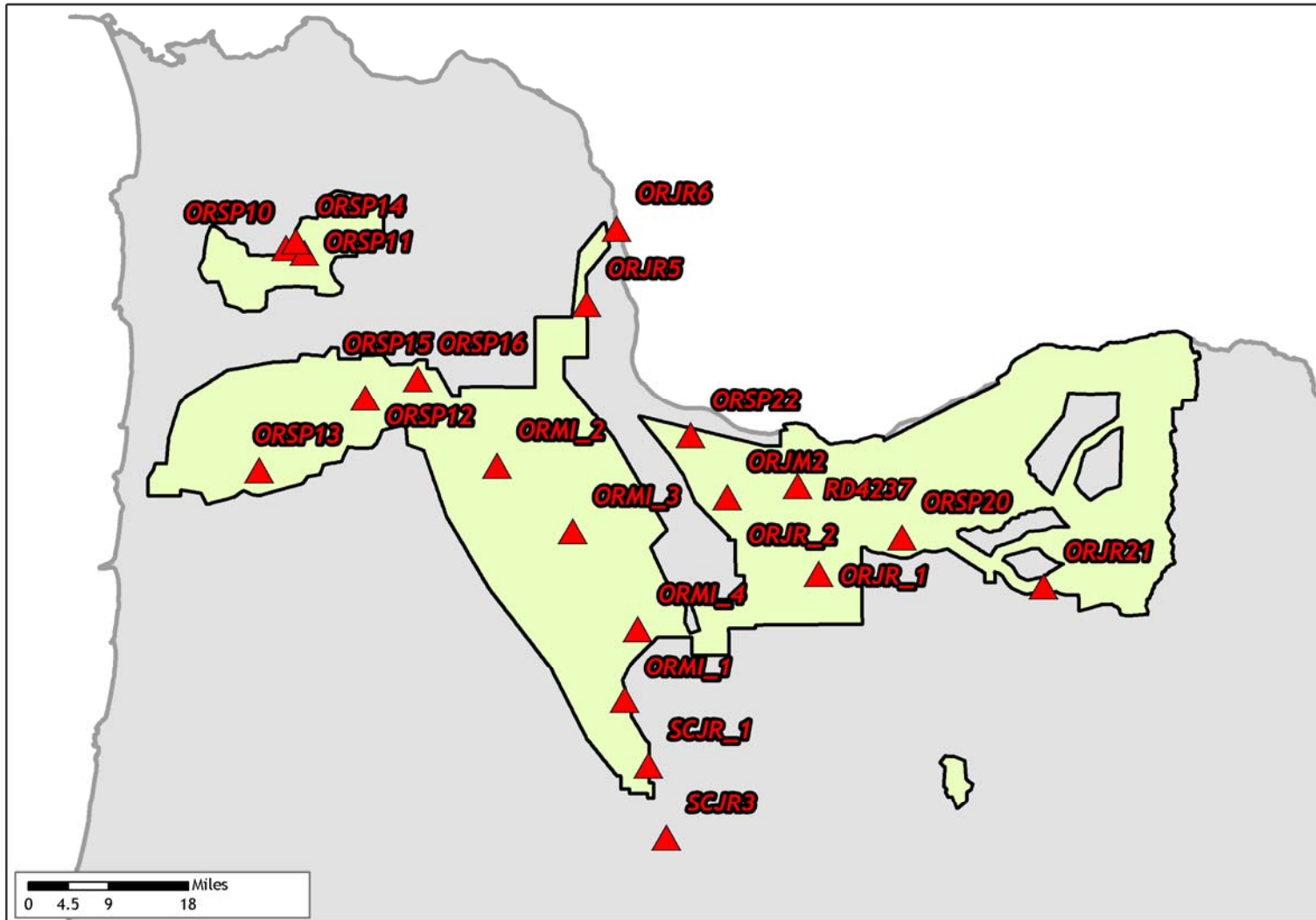**Figure 5.** Base station locations in the ODF and DOGAMI study areas.

Figure 6. RTK point locations in the ODF study areas; color images are NAIP Orthoimages, black and white image is 1.5-foot resolution intensity image derived from LiDAR data.
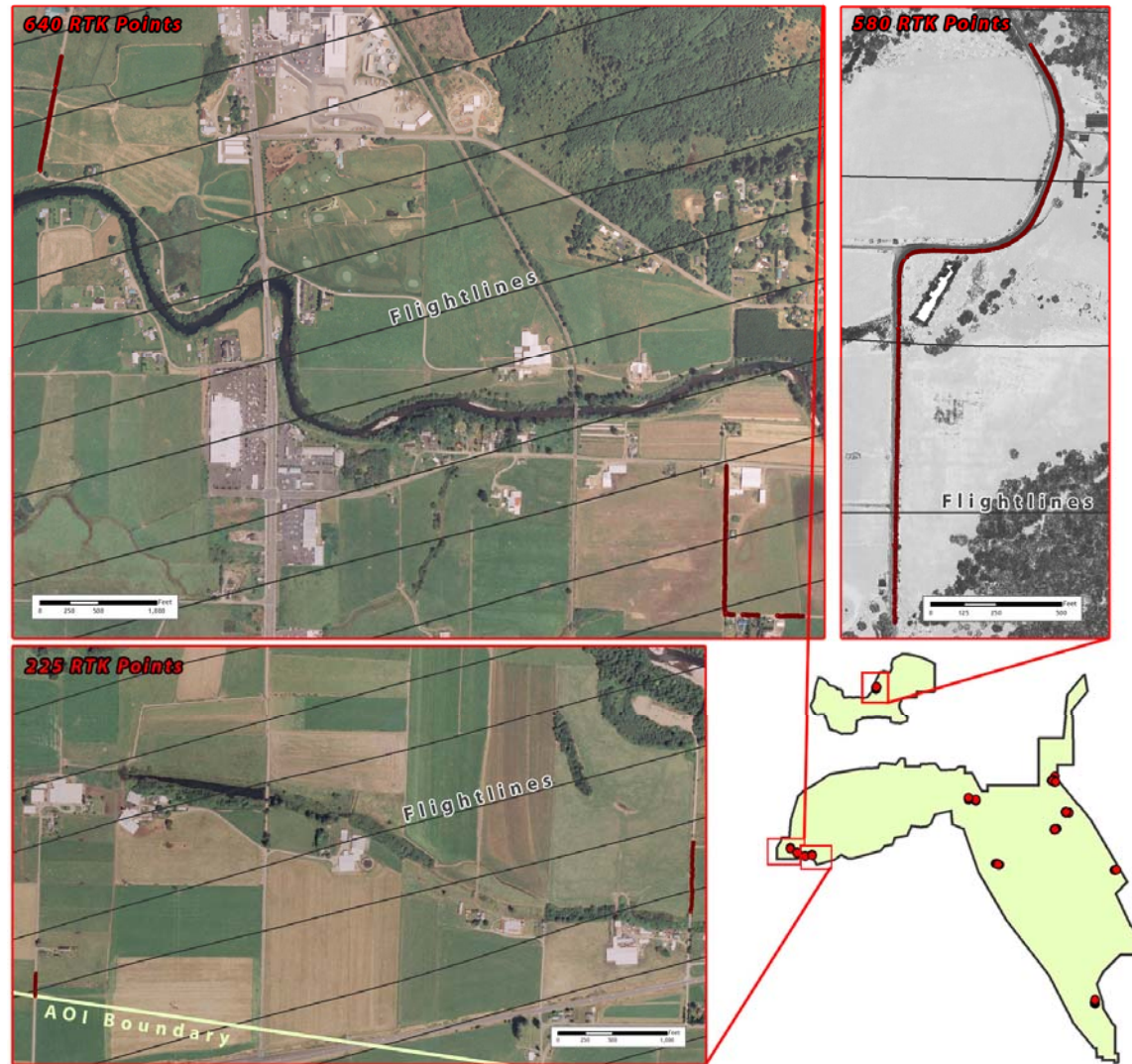
Figure 7. RTK point locations in the DOGAMI study areas; color images are NAIP Orthoimages.
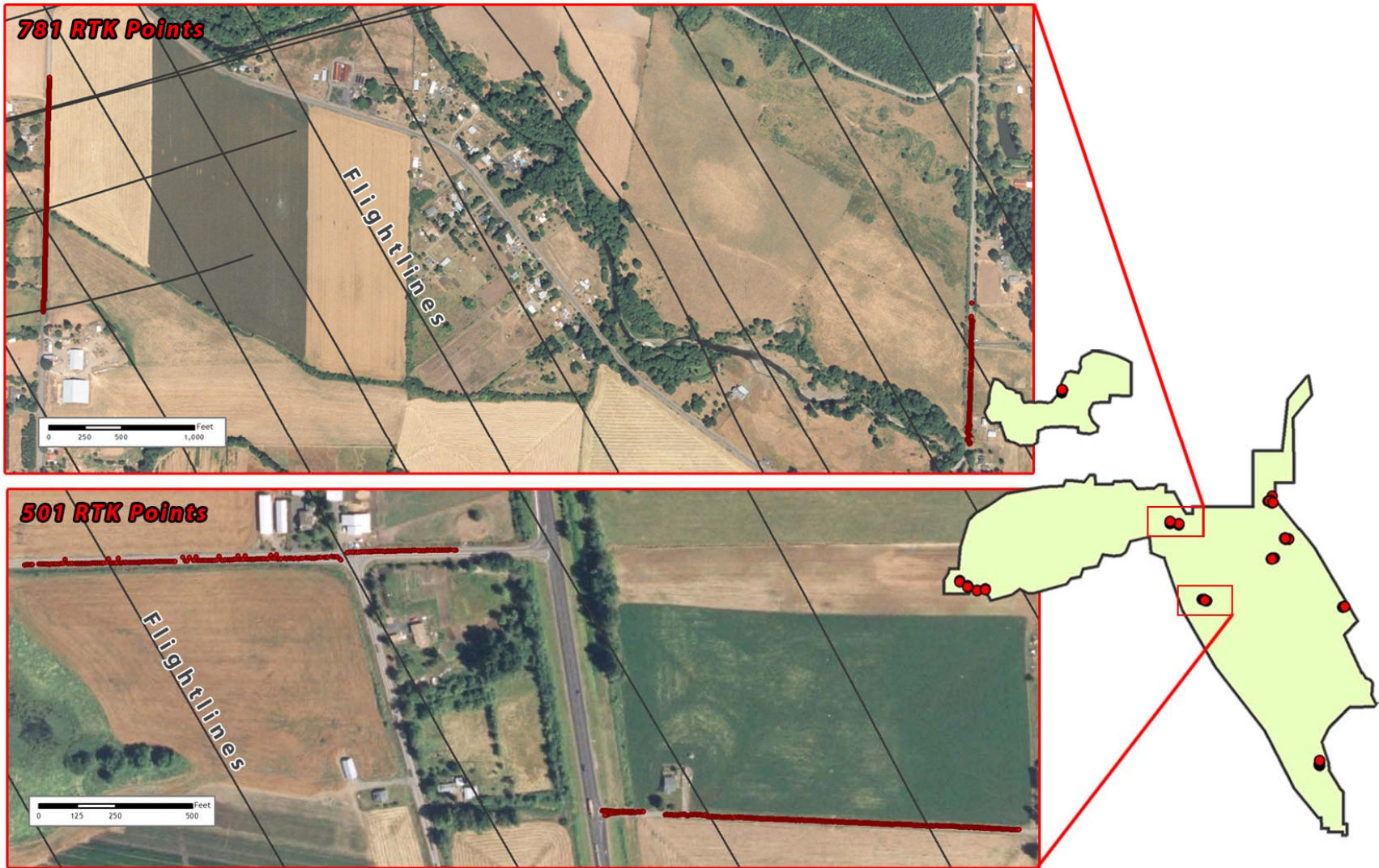

781 RTK Points

Flightlines

Feet
0   250   500   1,000

501 RTK Points

Flightlines

Feet
0   125   250   500

Figure 8. RTK point locations in the DOGAMI study areas; color images are NAIP Orthoimages.

LiDAR Remote Sensing Data: Department of Geology and Mineral Industries and Oregon Department of Forestry
Prepared by Watershed Sciences, Inc. *February 19, 2008*

Figure 9. RTK point locations in the DOGAMI study areas; color images are NAIP Orthoimages.

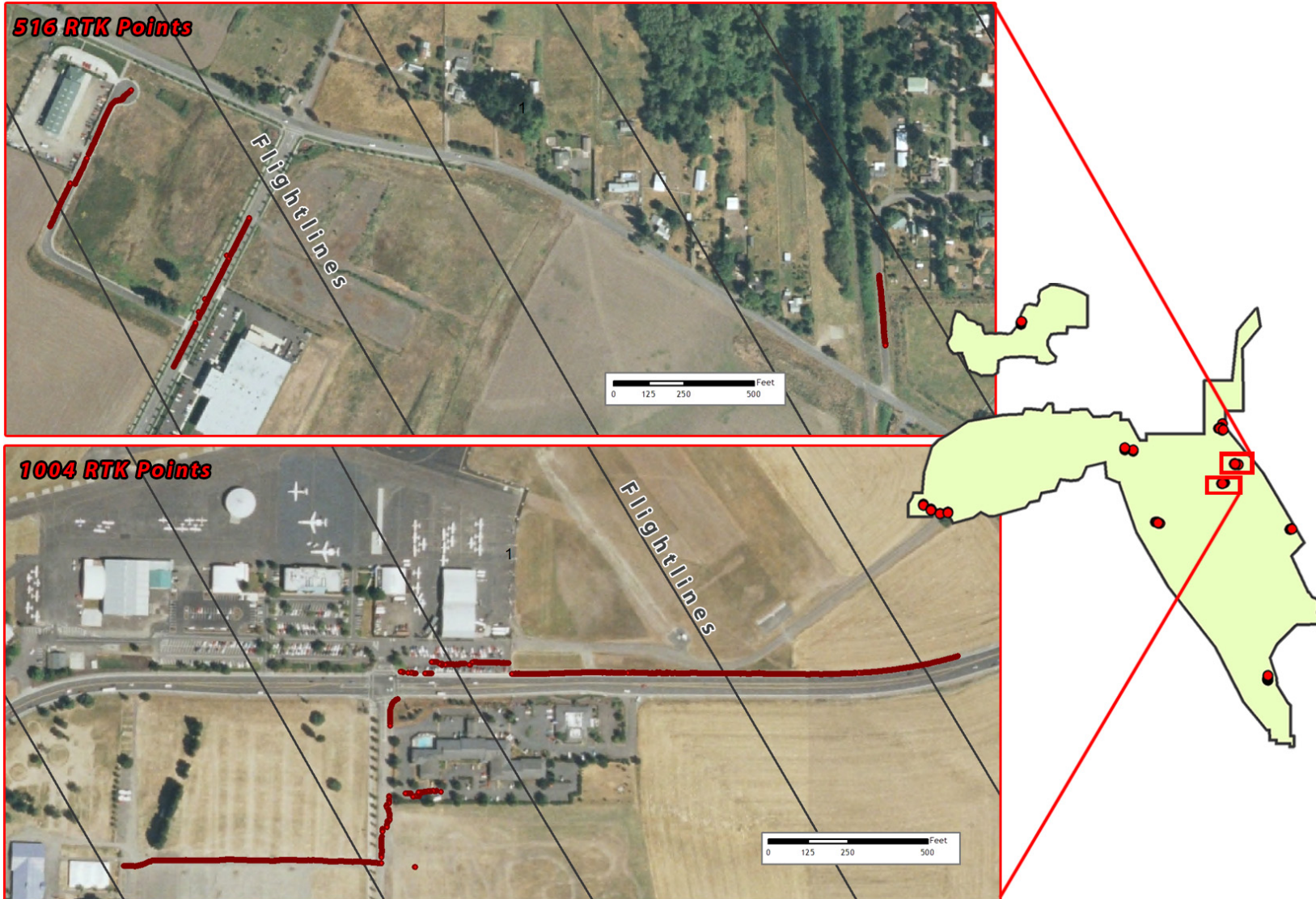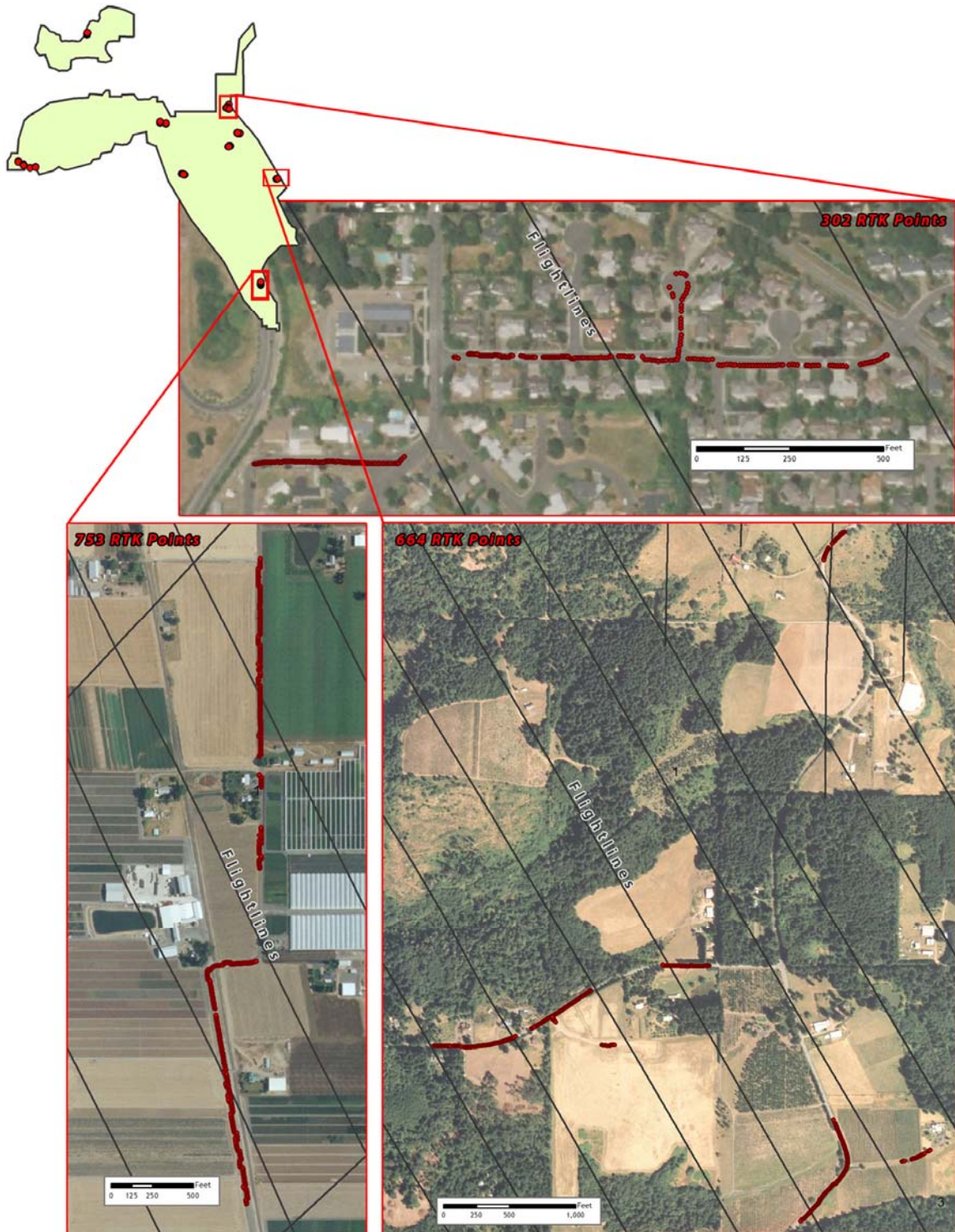**Figure 10.** RTK point locations in the DOGAMI study areas; color images are NAIP Orthoimages.

Figure 11. RTK point locations in the DOGAMI study areas; color images are NAIP Orthoimages.

Figure 12. RTK point locations in the DOGAMI study areas; color images are NAIP Orthoimages.
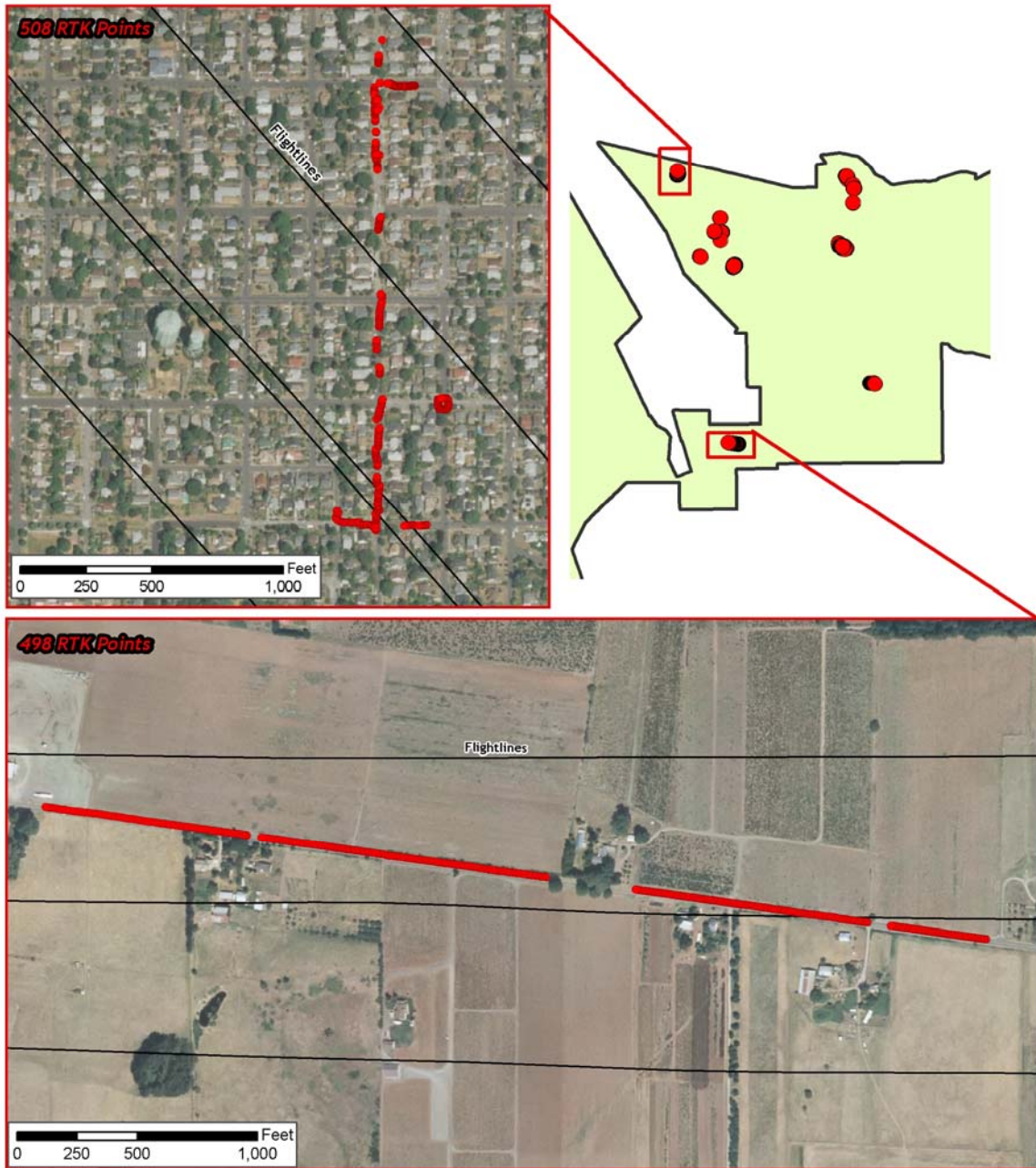
Figure 13. RTK point locations in the DOGAMI study areas; color images are NAIP Orthoimages.
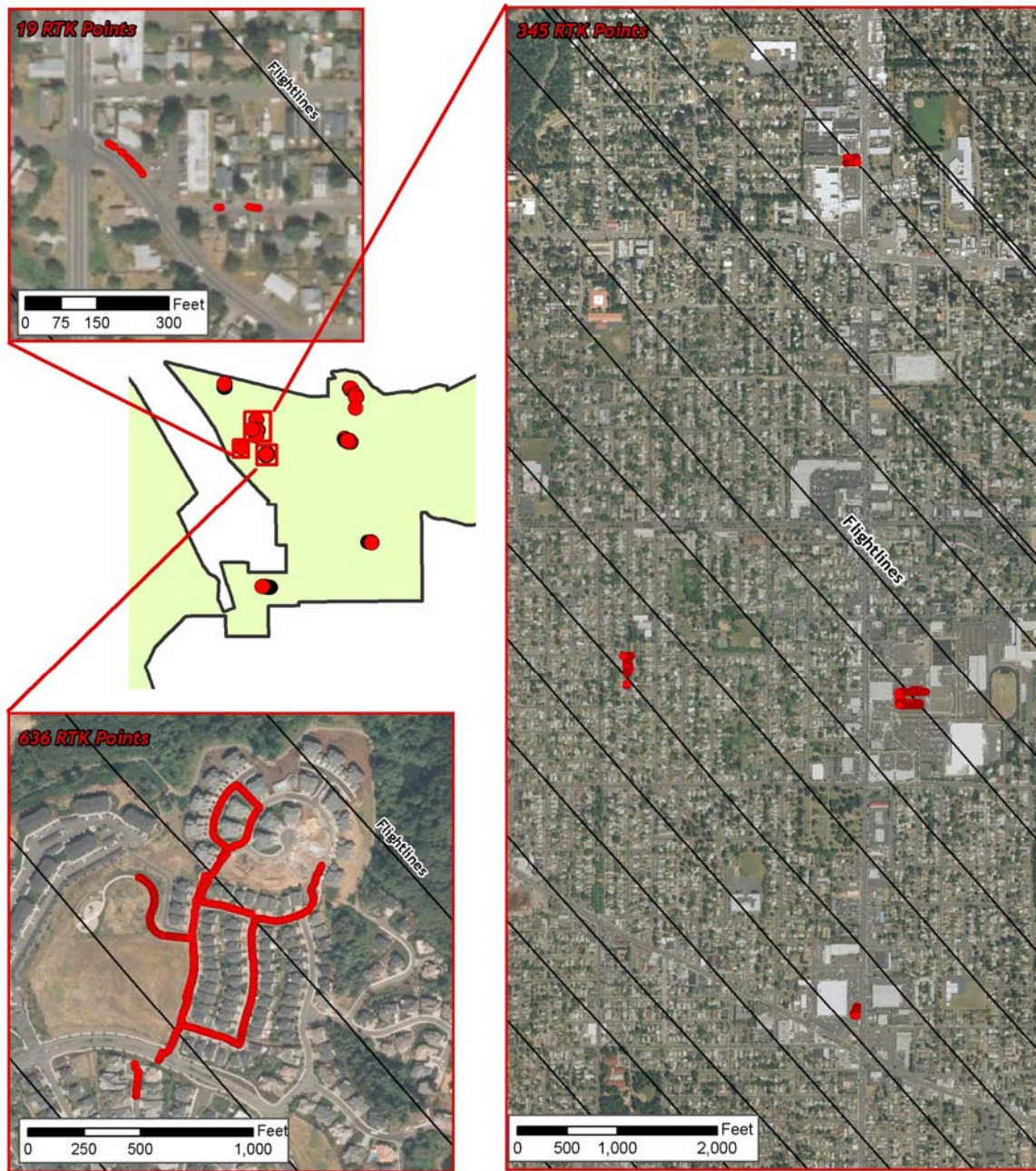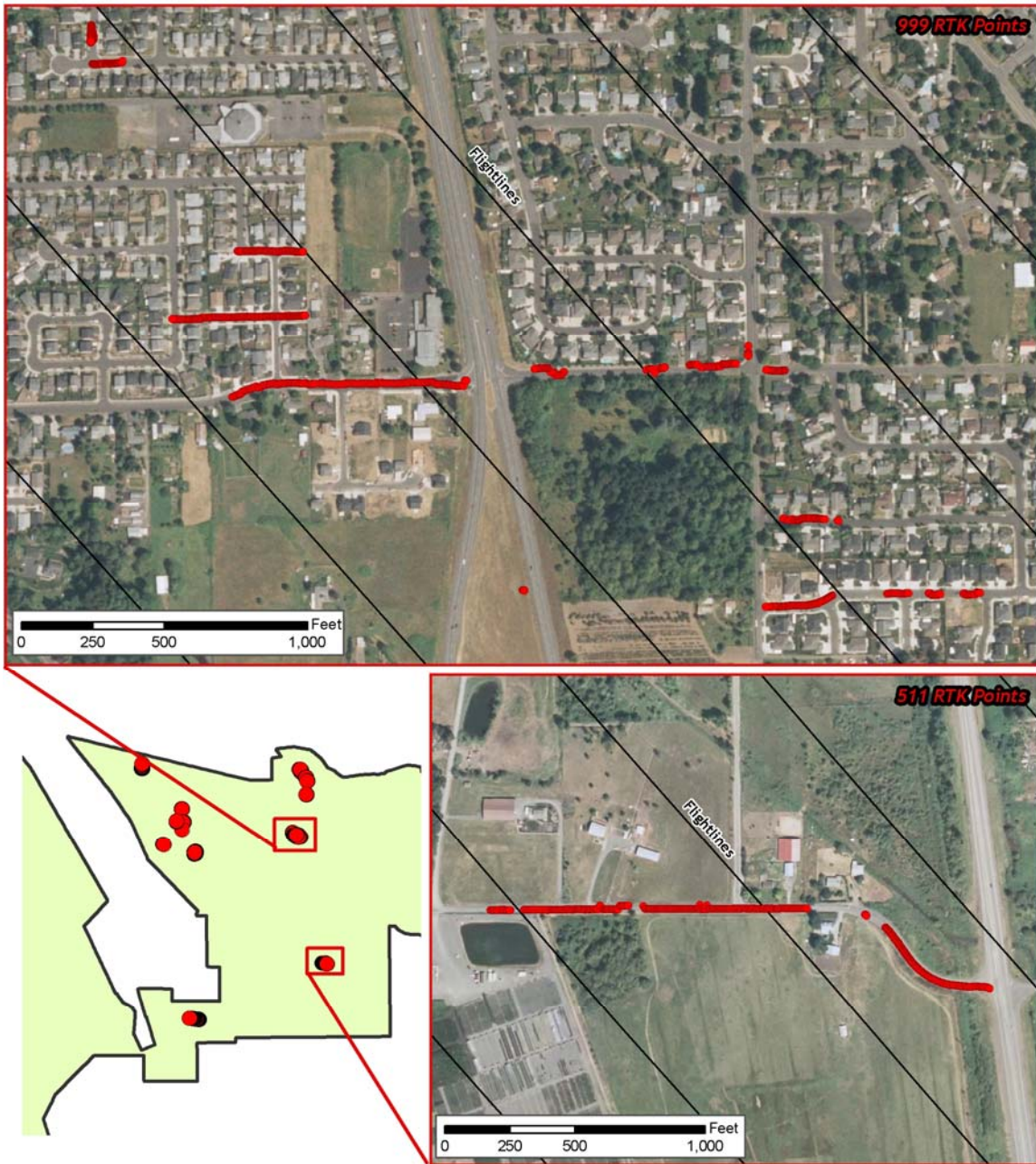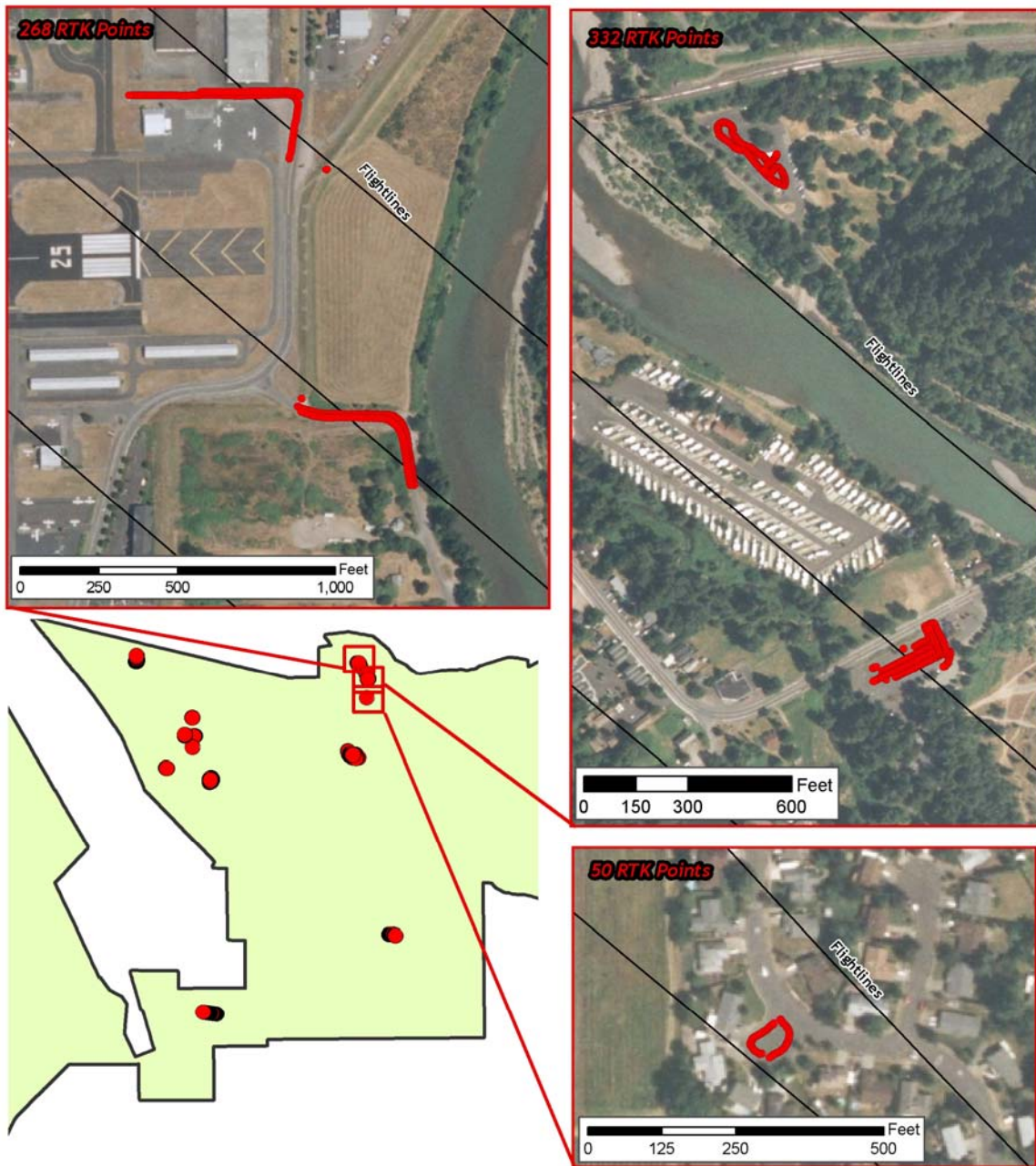
3. LiDAR Data Processing

3.1 Applications and Work Flow Overview

1. Resolve kinematic corrections for aircraft position data using kinematic aircraft GPS and static ground GPS data.
   Software: Waypoint GPS v.7.60

2. Develop a smoothed best estimate of trajectory (SBET) file that blends the post-processed aircraft position with attitude data. Sensor head position and attitude are calculated throughout the survey. The SBET data are used extensively for laser point processing.
   Software: IPAS v.1.0

3. Calculate laser point position by associating the SBET position to each laser point return time, scan angle, intensity, etc. Creates raw laser point cloud data for the entire survey in *.las (ASPRS v1.1) format.
   Software: ALS Post Processing Software

4. Import raw laser points into manageable blocks (less than 500 MB) to perform manual relative accuracy calibration and filter for pits/birds. Ground points are then classified for individual flight lines (to be used for relative accuracy testing and calibration).
   Software: TerraScan v.6.009

5. Using ground classified points per each flight line, the relative accuracy is tested. Automated line-to-line calibrations are then performed for system attitude parameters (pitch, roll, heading), mirror flex (scale) and GPS/IMU drift. Calibrations are performed on ground classified points from paired flight lines. Every flight line is used for relative accuracy calibration.
   Software: TerraMatch v.6.009

6. Position and attitude data are imported. Resulting data are classified as ground and non-ground points. Statistical absolute accuracy is assessed via direct comparisons of ground classified points to ground RTK survey data. Data are then converted to orthometric elevations (NAVD88) by applying a Geoid03 correction. Ground models are created as a triangulated surface and exported as ArcInfo ASCII grids at a 3-foot pixel resolution.
   Software: TerraScan v.6.009, ArcMap v9.2

3.2 Aircraft Kinematic GPS and IMU Data

LiDAR survey datasets are referenced to 1 Hz static ground GPS data collected over pre-surveyed monuments with known coordinates. While surveying, the aircraft collects 2 Hz kinematic GPS data. The onboard inertial measurement unit (IMU) collects 200 Hz aircraft attitude data. Waypoint GPS v.7.60 is used to process the kinematic corrections for the aircraft. The static and kinematic GPS data are then post-processed after the survey to obtain an accurate GPS solution and aircraft positions. IPAS v.1.0 is used to develop a trajectory file that includes corrected aircraft position and attitude information. The trajectory data for the entire flight survey session are incorporated into a final smoothed best estimated trajectory (SBET) file that contains accurate and continuous aircraft positions and attitudes.

3.3 Laser Point Processing

Laser point coordinates are computed using the IPAS and ALS Post Processor software suites based on independent data from the LiDAR system (pulse time, scan angle), and aircraft trajectory data (SBET). Laser point returns (first through fourth) are assigned an associated (x, y, z) coordinate along with unique intensity values (0-255). The data are output into large LAS v. 1.1 files; each point maintains the corresponding scan angle, return number (echo), intensity, and x, y, z (easting, northing, and elevation) information.

These initial laser point files are too large to process. To facilitate laser point processing, bins (polygons) are created to divide the dataset into manageable sizes (< 500 MB). Flightlines and LiDAR data are then reviewed to ensure complete coverage of the study area and positional accuracy of the laser points.

Once the laser point data are imported into bins in TerraScan, a manual calibration is performed to assess the system offsets for pitch, roll, heading and mirror scale. Using a geometric relationship developed by Watershed Sciences, each of these offsets is resolved and corrected if necessary.

The LiDAR points are then filtered for noise, pits and birds by screening for absolute elevation limits, isolated points and height above ground. Each bin is then inspected for pits and birds manually; spurious points are removed. For a bin containing approximately 7.5-9.0 million points, an average of 50-100 points are typically found to be artificially low or high. These spurious non-terrestrial laser points must be removed from the dataset. Common sources of non-terrestrial returns are clouds, birds, vapor, and haze.

The internal calibration is refined using TerraMatch. Points from overlapping lines are tested for internal consistency and final adjustments are made for system misalignments (i.e., pitch, roll, heading offsets and mirror scale). Automated sensor attitude and scale corrections yield 3-5 cm improvements in the relative accuracy. Once the system misalignments are corrected, vertical GPS drift is then resolved and removed per flight line, yielding a slight improvement (<1 cm) in relative accuracy. At this point in the workflow, data have passed a robust calibration designed to reduce inconsistencies from multiple sources (i.e. sensor attitude offsets, mirror scale, GPS drift) using a procedure that is comprehensive (i.e. uses all of the overlapping survey data). Relative accuracy screening is complete.

The TerraScan software suite is designed specifically for classifying near-ground points (Soininen, 2004). The processing sequence begins by 'removing' all points that are not 'near' the earth based on geometric constraints used to evaluate multi-return points. The resulting bare earth (ground) model is visually inspected and additional ground point modeling is performed in site-specific areas (over a 50-meter radius) to improve ground detail. This is only done in areas with known ground modeling deficiencies, such as: bedrock outcrops, cliffs, deeply incised stream banks, and dense vegetation. In some cases, ground point classification includes known vegetation (i.e., understory, low/dense shrubs, etc.) and these points are reclassified as non-grounds. Ground surface rasters are developed from triangulated irregular networks (TINs) of ground points.

4. LiDAR Accuracy and Resolution

4.1 Laser Point Accuracy

Laser point absolute accuracy is largely a function of internal consistency (measured as relative accuracy) and laser noise:

- **Laser Noise**: For any given target, laser noise is the breadth of the data cloud per laser return (i.e., last, first, etc.). Lower intensity surfaces (roads, rooftops, still/calm water) experience higher laser noise. The laser noise range for this mission is approximately 0.02 meters.

- **Relative Accuracy**: Internal consistency refers to the ability to place a laser point in the same location over multiple flight lines, GPS conditions, and aircraft attitudes.

- **Absolute Accuracy**: RTK GPS measurements taken in the study areas compared to LiDAR point data.

Statements of statistical accuracy apply to fixed terrestrial surfaces only, not to free-flowing or standing water surfaces, moving automobiles, et cetera.

Table 2. LiDAR accuracy is a combination of several sources of error. These sources of error are cumulative. Some error sources that are biased and act in a patterned displacement can be resolved in post processing.

Type of Error	Source	Post Processing Solution
GPS (Static/Kinematic)	Long Base Lines	None
	Poor Satellite Constellation	None
	Poor Antenna Visibility	Reduce Visibility Mask
Relative Accuracy	Poor System Calibration	Recalibrate IMU and sensor offsets/settings
	Inaccurate System	None
Laser Noise	Poor Laser Timing	None
	Poor Laser Reception	None
	Poor Laser Power	None
	Irregular Laser Shape	None

4.1.1 Relative Accuracy

Relative accuracy refers to the internal consistency of the data set and is measured as the divergence between points from different flight lines within an overlapping area. Divergence is most apparent when flight lines are opposing. When the LiDAR system is well calibrated the line to line divergence is low (<10 cm). Internal consistency is affected by system attitude offsets (pitch, roll and heading), mirror flex (scale), and GPS/IMU drift.

Operational measures taken to improve relative accuracy:

1. <u>Low Flight Altitude</u>: Terrain following was targeted at a flight altitude of 900 meters above ground level (AGL). Laser horizontal errors are a function of flight altitude above ground (i.e., ~ 1/3000th AGL flight altitude). Lower flight altitudes decrease laser noise on surfaces with even the slightest relief.
2. <u>Focus Laser Power at narrow beam footprint</u>: A laser return must be received by the system above a power threshold to accurately record a measurement. The strength of the laser return is a function of laser emission power, laser footprint, flight altitude and the reflectivity of the target. While surface reflectivity cannot be controlled, laser power can be increased and low flight altitudes can be maintained.
3. <u>Reduced Scan Angle</u>: Edge-of-scan data can become inaccurate. The scan angle was reduced to a maximum of ±14° from nadir, creating a narrow swath width and greatly reducing laser shadows from trees and buildings.
4. <u>Quality GPS</u>: Flights took place during optimal GPS conditions (e.g., 6 or more satellites and PDOP [Position Dilution of Precision] less than 3.0). Before each flight, the PDOP was determined for the survey day. During all flight times, a dual frequency DGPS base station recording at 1–second epochs was utilized and a maximum baseline length between the aircraft and the control points was less than 19 km (11.5 miles) at all times.
5. <u>Ground Survey</u>: Ground survey point accuracy (i.e., <1.5 cm RMSE) occurs during optimal PDOP ranges and targets a minimal baseline distance of 4 miles between GPS rover and base. Robust statistics are, in part, a function of sample size (n) and distribution. The ground survey collected 10,131 RTK points that are distributed throughout multiple flight lines across the study areas.
6. <u>50% Side-Lap (100% Overlap)</u>: Overlapping areas are optimized for relative accuracy testing. Laser shadowing is minimized to help increase target acquisition from multiple scan angles. Ideally, with a 50% side-lap, the most nadir portion of one flight line coincides with the edge (least nadir) portion of overlapping flight lines. A minimum of 50% side-lap with terrain-followed acquisition prevents data gaps.
7. <u>Opposing Flight Lines</u>: All overlapping flight lines are opposing. Pitch, roll and heading errors are amplified by a factor of two relative to the adjacent flight line(s), making misalignments easier to detect and resolve.

Relative Accuracy Calibration Methodology

1. <u>Manual System Calibration</u>: Calibration procedures for each mission require solving geometric relationships that relate measured swath-to-swath deviations to misalignments of system attitude parameters. Corrected scale, pitch, roll and heading offsets are calculated and applied to resolve misalignments. The raw divergence between lines is computed after the manual calibration is completed and reported for each study area.

2. <u>Automated Attitude Calibration</u>: All data are tested and calibrated using TerraMatch automated sampling routines. Ground points are classified for each individual flight line and used for line-to-line testing. *The resulting overlapping ground points (per line) total over 9 billion points from which to compute and refine relative accuracy*. System misalignment offsets (pitch, roll and heading) and mirror scale are solved for each individual mission. The application of attitude misalignment offsets (and mirror scale) occurs for each individual mission. The data from each mission are then blended when imported together to form the entire area of interest.

3. <u>Automated Z Calibration</u>: Ground points per line are utilized to calculate the vertical divergence between lines caused by vertical GPS drift. Automated Z calibration is the final step employed for relative accuracy calibration.

Relative Accuracy Calibration Results (see Figures below)

Relative accuracies have been determined for all portions of the DOGAMI & ODF study areas acquired to date; the statistics are based on the comparison of 1,158 flightlines and over 9 billion points. For flightline coverage, see **Figure 4** in Section 2.1.

- o   Project Average = 0.054 m
- o   Median Relative Accuracy = 0.075 m
- o   1σ Relative Accuracy = 0.101 m
- o   2σ Relative Accuracy = 0.182 m

Figure 14. Distribution of relative accuracies per flight line, non slope-adjusted.
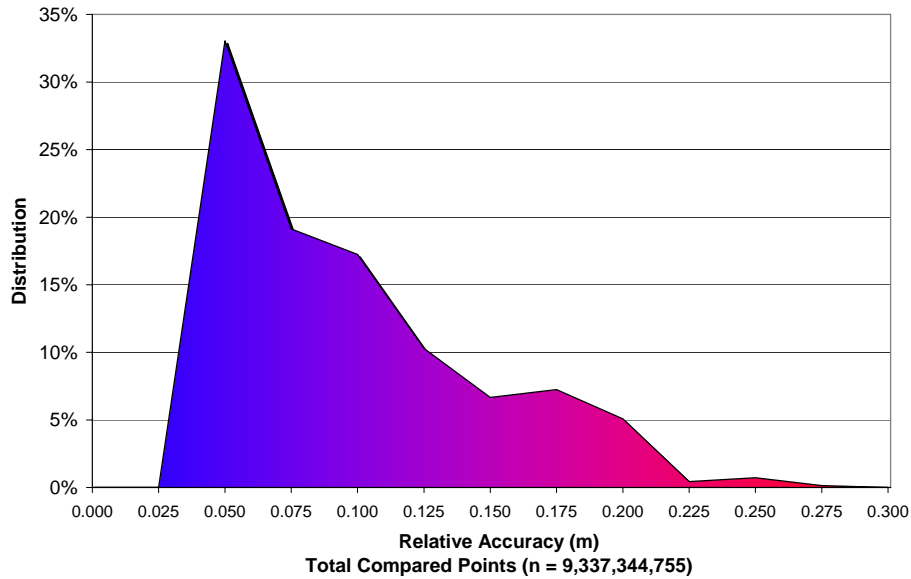
Figure 15. Statistical relative accuracies, non slope-adjusted.

LiDAR Remote Sensing Data: Department of Geology and Mineral Industries and Oregon Department of Forestry
Prepared by Watershed Sciences, Inc.   *February 19, 2008*
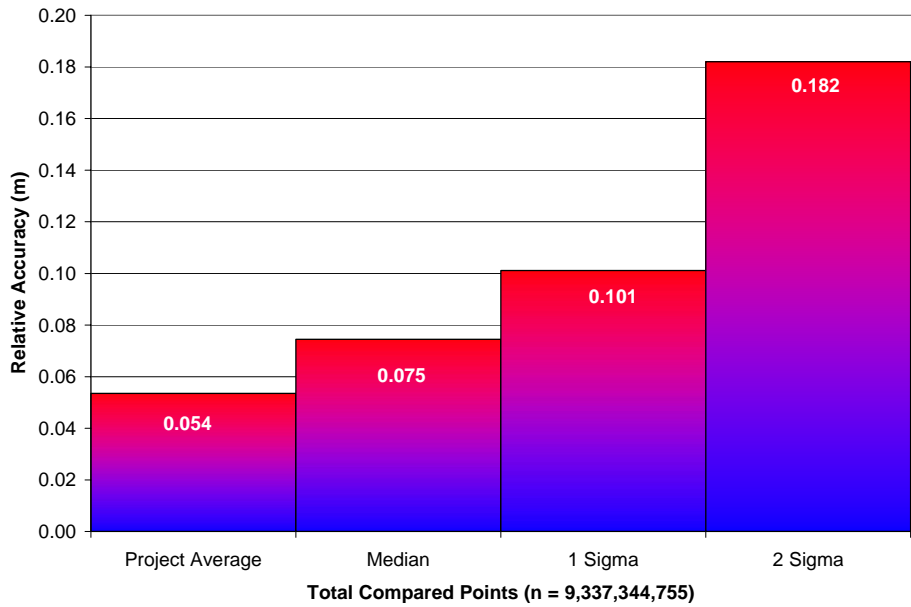
4.1.2 Absolute Accuracy

The final quality control measure is a statistical accuracy assessment that compares known RTK ground survey points to the closest laser point. Accuracy statistics are reported in **Table 3** and shown in Figures **16-17**. Accuracy statistics have been developed for the areas shown in **Figures 6-13** in Section 2.2.

Table 3. Absolute Accuracy – Deviation between laser points and RTK survey points.

Sample Size (n): 10,131	
Root Mean Square Error (RMSE): 0.11feet	
Standard Deviations	**Deviations**
1 sigma (σ): 0.11 feet	**Minimum Δz:** -0.52 feet
2 sigma (σ): 0.23 feet	**Maximum Δz:** 0.45 feet
	Average Δz: 0.00 feet

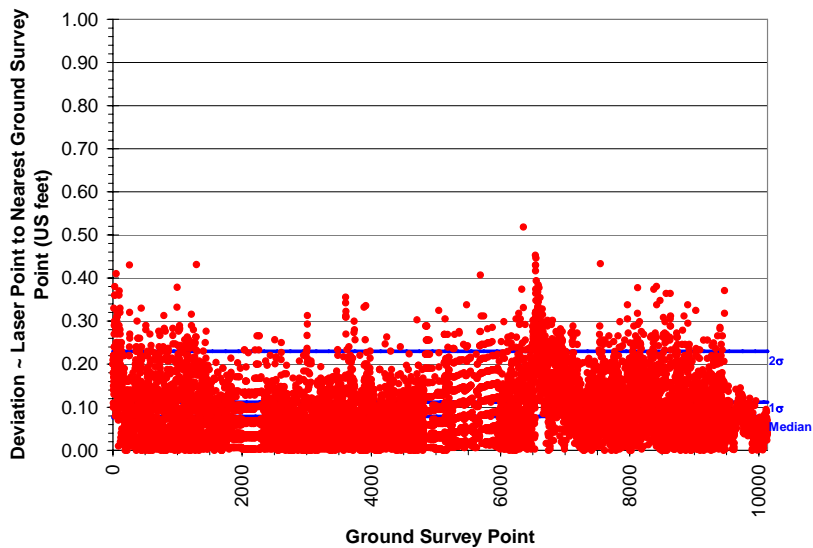**Figure 16. Study Area:** Histogram Statistics
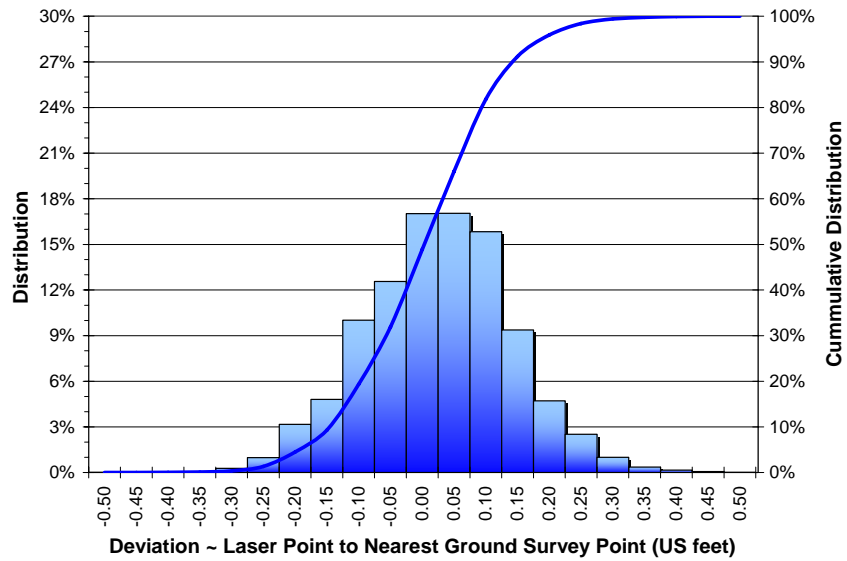
Figure 17. Study Area: Point Absolute Deviation Statistics

4.2 Data Density/Resolution

Some types of surfaces (i.e., dense vegetation or water) may return fewer pulses than the laser originally emitted. Therefore, the delivered density can be less than the native density and lightly variable according to distributions of terrain, land cover and water bodies. Density histograms and maps (Figures 18-25) have been calculated based on first return laser point density and ground-classified laser point density.

- The total delivered density for ODF's AOIs (complete) is 0.72 points per square foot (7.71 points per square meter, based on first return pulses only).
- The total delivered density for all delivered data for the Portland Area to date is 0.64 points per square foot (6.91 points per square meter, based on first return pulses only).

4.2.1 First Return Laser Pulses per Square Foot

Figure 18. Histogram of first return laser point data density in both of **ODF's AOIs**, per 0.75' USGS Quad. Project area average: 0.72 points per square foot / 7.71 points per square meter.
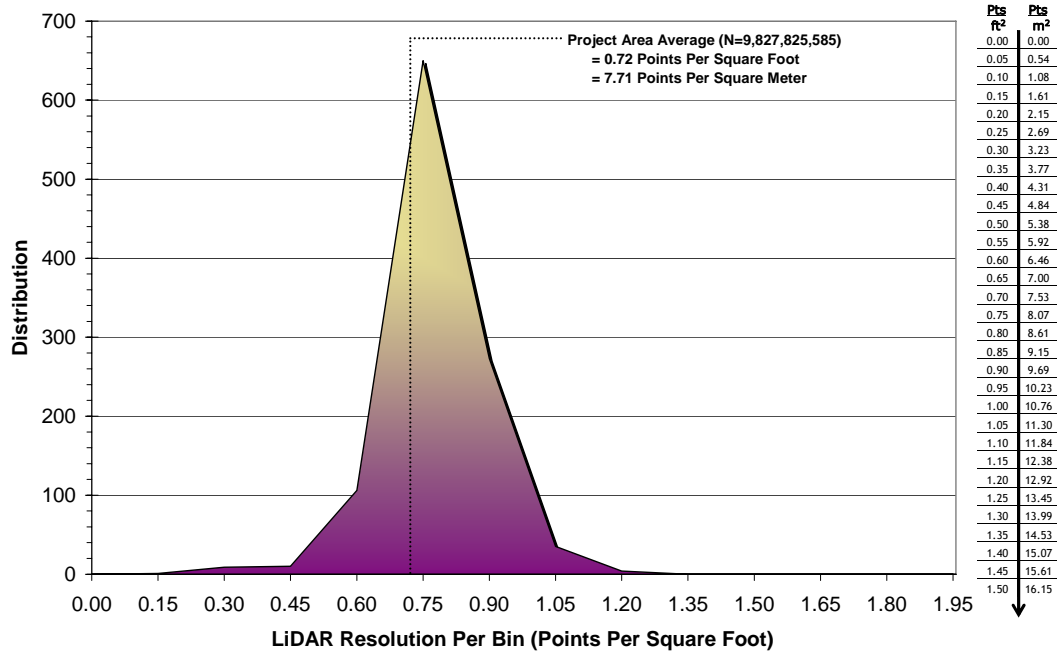

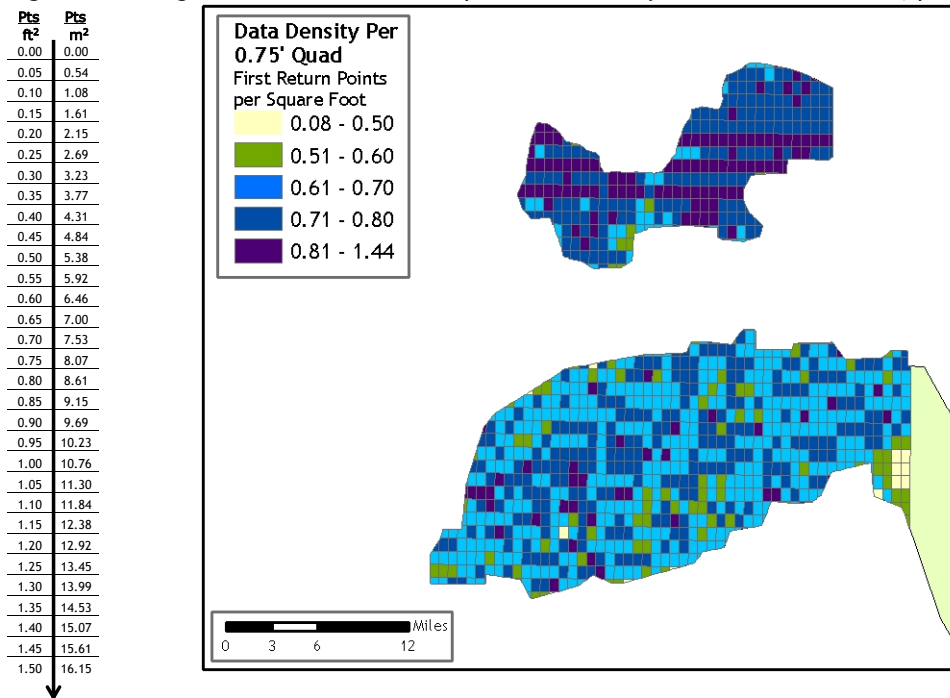**Figure 19.** Image shows first return laser point data density in both of **ODF's AOIs,** per 0.75' USGS Quad.

Figure 20. Histogram of first return laser point data density in **all Portland Area quads delivered to date**, per 0.75' USGS Quad. Project area average: 0.64 points per square foot / 6.91 points per square meter.
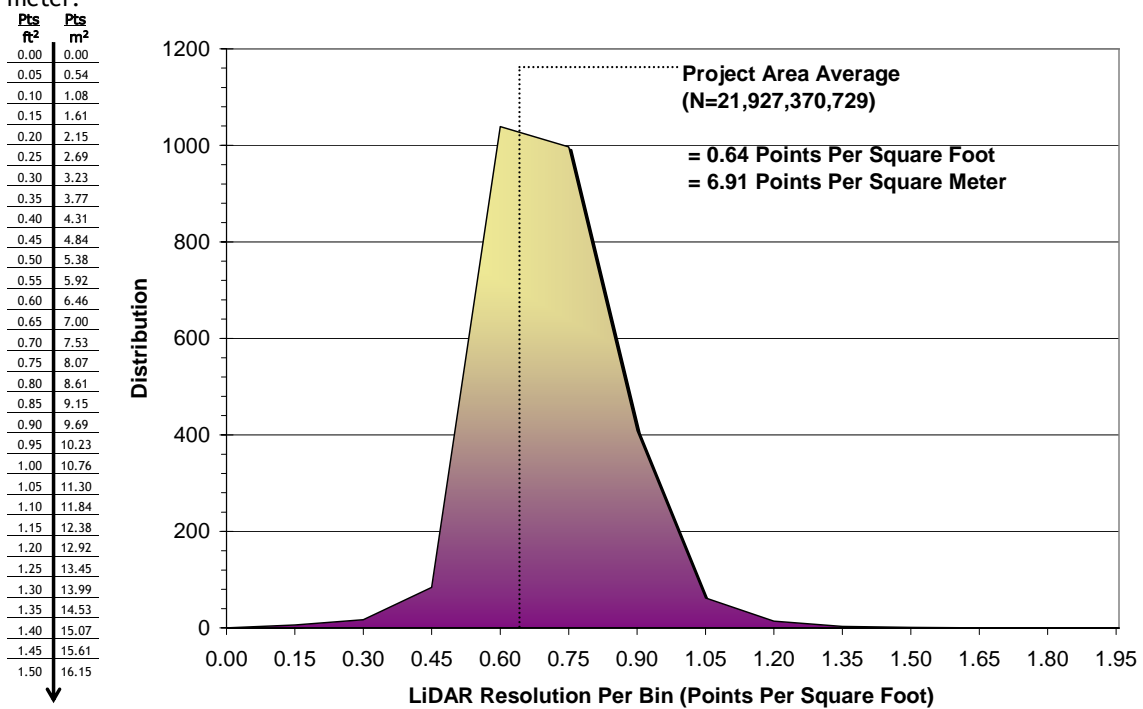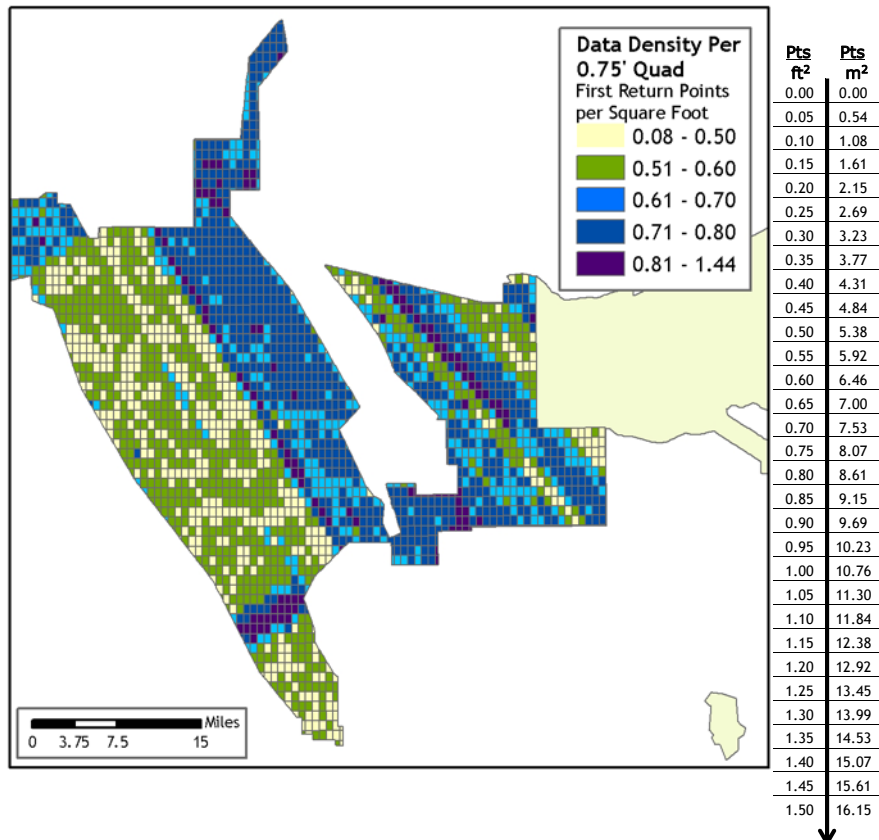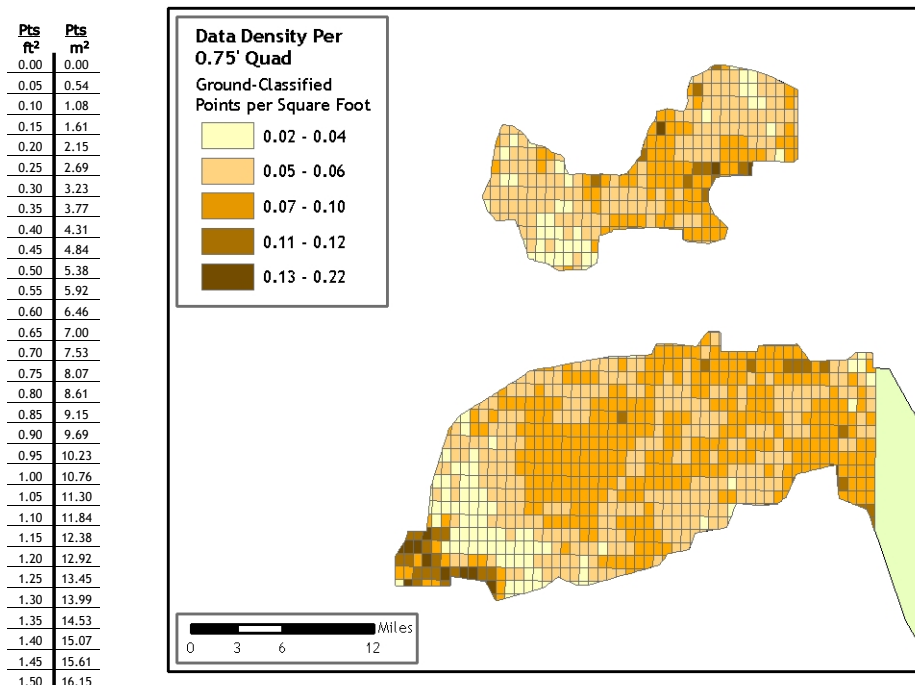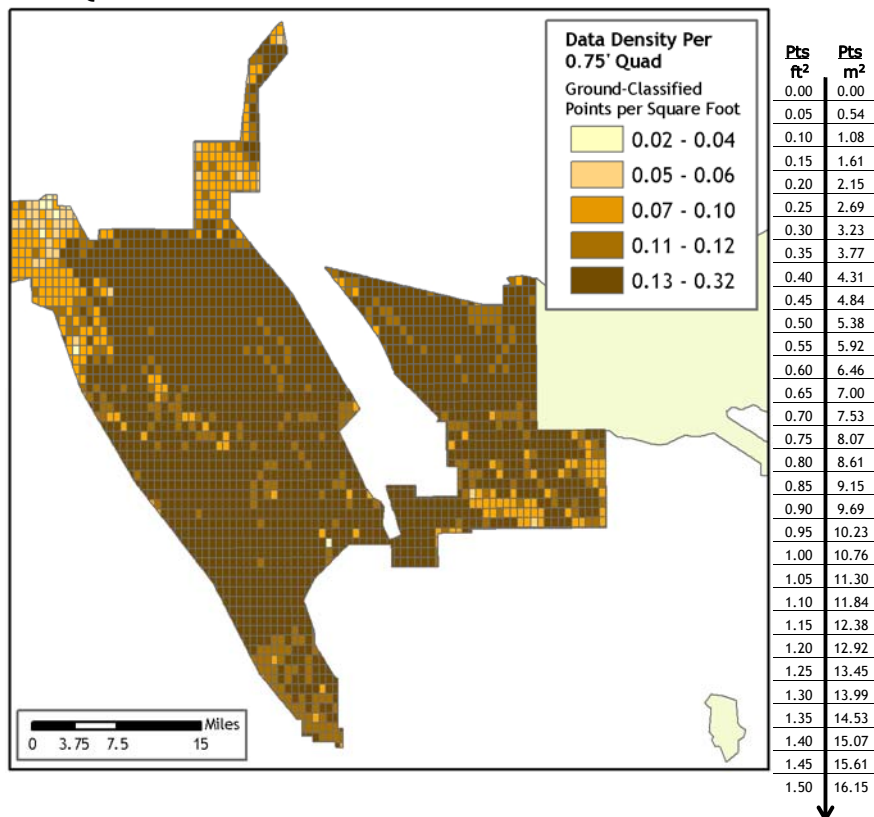
Pts ft²	Pts m²
0.00	0.00
0.05	0.54
0.10	1.08
0.15	1.61
0.20	2.15
0.25	2.69
0.30	3.23
0.35	3.77
0.40	4.31
0.45	4.84
0.50	5.38
0.55	5.92
0.60	6.46
0.65	7.00
0.70	7.53
0.75	8.07
0.80	8.61
0.85	9.15
0.90	9.69
0.95	10.23
1.00	10.76
1.05	11.30
1.10	11.84
1.15	12.38
1.20	12.92
1.25	13.45
1.30	13.99
1.35	14.53
1.40	15.07
1.45	15.61
1.50	16.15

Project Area Average
(N=21,927,370,729)

= 0.64 Points Per Square Foot
= 6.91 Points Per Square Meter

Distribution

LiDAR Resolution Per Bin (Points Per Square Foot)

Figure 21. Image shows first return laser point data density in **all Portland Area quads delivered to date**, per 0.75' USGS Quad.

Data Density Per 0.75' Quad
First Return Points per Square Foot

- 0.08 - 0.50
- 0.51 - 0.60
- 0.61 - 0.70
- 0.71 - 0.80
- 0.81 - 1.44

Pts ft²	Pts m²
0.00	0.00
0.05	0.54
0.10	1.08
0.15	1.61
0.20	2.15
0.25	2.69
0.30	3.23
0.35	3.77
0.40	4.31
0.45	4.84
0.50	5.38
0.55	5.92
0.60	6.46
0.65	7.00
0.70	7.53
0.75	8.07
0.80	8.61
0.85	9.15
0.90	9.69
0.95	10.23
1.00	10.76
1.05	11.30
1.10	11.84
1.15	12.38
1.20	12.92
1.25	13.45
1.30	13.99
1.35	14.53
1.40	15.07
1.45	15.61
1.50	16.15

Miles
0 3.75 7.5 15

4.2.2 Classified Ground Points per Square Foot

Ground classifications are derived from ground surface modeling. Supervised classifications were performed by reseeding of the ground model where it is determined that the ground model has failed, usually under dense vegetation and/or at breaks in terrain, steep slopes and at bin boundaries. Ground point density information is summarized below.

Figure 22. Histogram of ground-classified laser point data density in both **ODF's AOIs**, per 0.75' USGS Quad. Project area average: 0.07 points per square foot / 0.71 points per square meter.
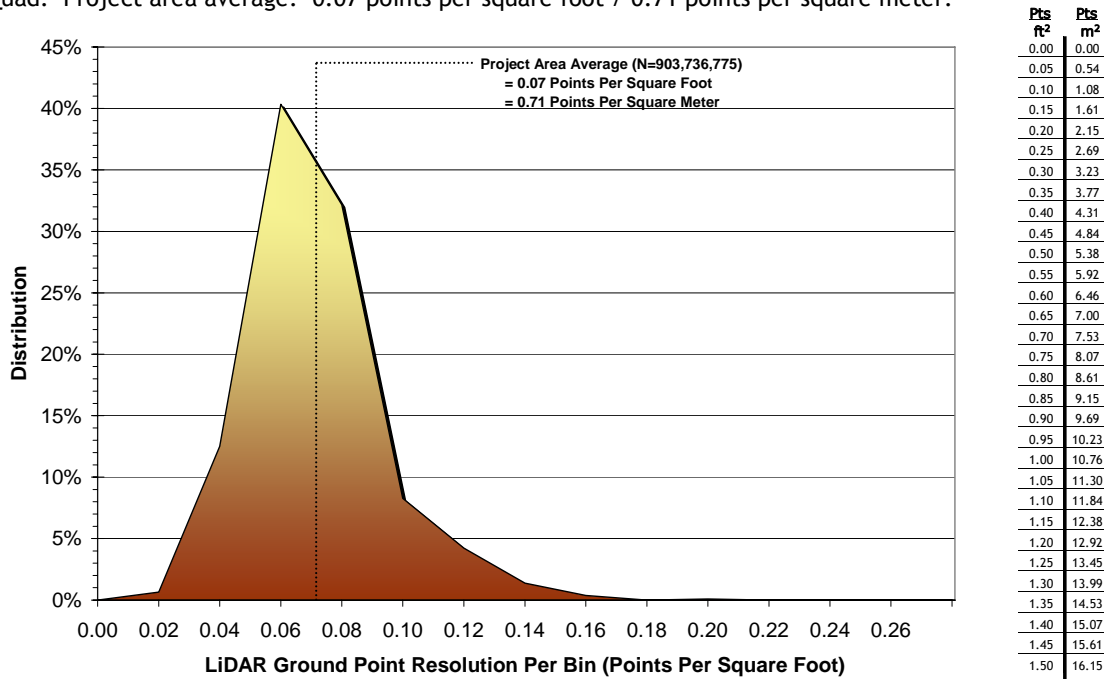
Figure 23. Image shows ground-classified laser point data density per 0.75' USGS Quad in both **ODF's AOIs**.

LiDAR Remote Sensing Data: Department of Geology and Mineral Industries and Oregon Department of Forestry
Prepared by Watershed Sciences, Inc.   *February 19, 2008*

Figure 24. Histogram of ground-classified laser point data density in **all Portland Area quads delivered to date**, per 0.75' USGS Quad. Project area average: 0.13 points per square foot / 1.42 points per square meter.
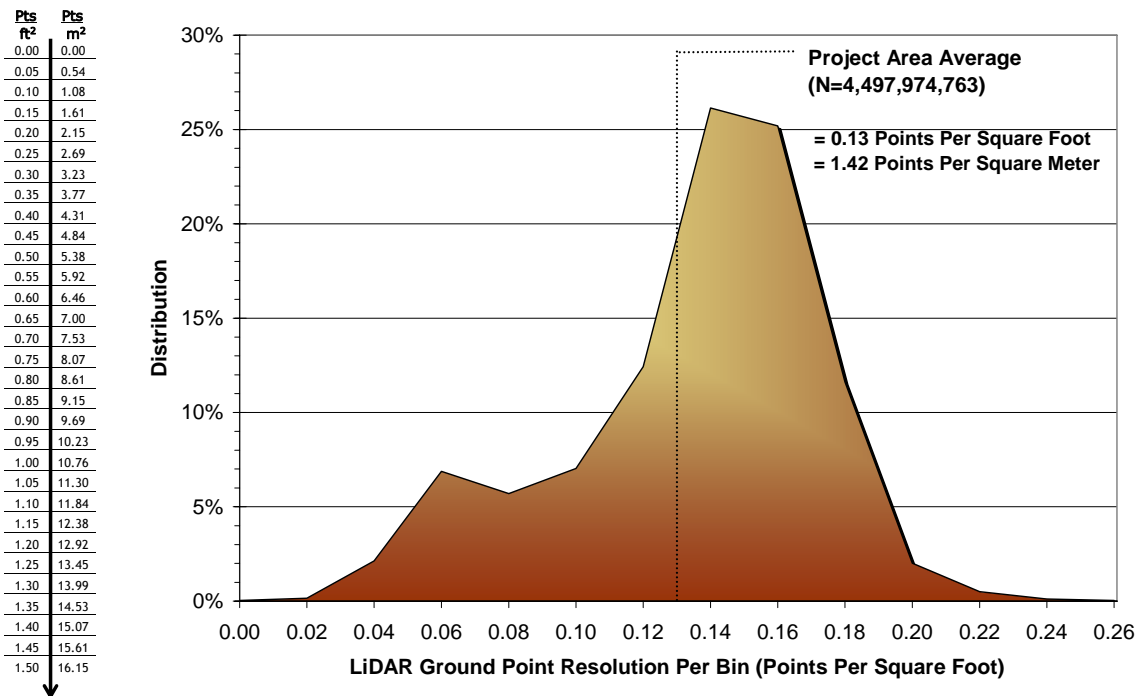
Figure 25. Image shows ground-classified laser point data density in **all Portland Area quads delivered to date**, per 0.75' USGS Quad.

LiDAR Remote Sensing Data: Department of Geology and Mineral Industries and Oregon Department of Forestry
Prepared by Watershed Sciences, Inc.   *February 19, 2008*

5. Deliverables

5.1 Point Data (per 0.75' USGS Quad)

Data Fields: Number, X, Y, Z, Intensity, ReturnNumber, NumReturns, ScanDirection, EdgeOfFlightLine, Class, ScanAngleRank, FileMarker, UserBitField, GPSTime

- LAS v 1.1 Format
- ASCII Format
- Smoothed Best Estimate of Trajectory Point Files in ASCII format

5.2 Vector Data

- Total Area Flown
  - 7.5-minute quadrangle delineation in shapefile format
  - 0.75-minute quadrangle delineation in shapefile format (See **Figure 26** below for illustration)

5.3 Raster Data

- ESRI GRID of Bare Earth Modeled LiDAR data Points (3-foot resolution) delivered in 7.5' USGS Quad Delineation
- ESRI GRID of Above Ground Modeled LiDAR data Points (3-foot resolution) delivered in 7.5' USGS Quad Delineation
- Intensity Images in GeoTIFF format (1.5-foot resolution) delivered per 0.75' Quad

5.4 Data Report

- Full Report containing introduction, methodology, and accuracy.
  - Word Format (*.doc)
  - PDF Format (*.pdf)

Figure 26. 0.75' USGS Quad Delineation Naming Convention
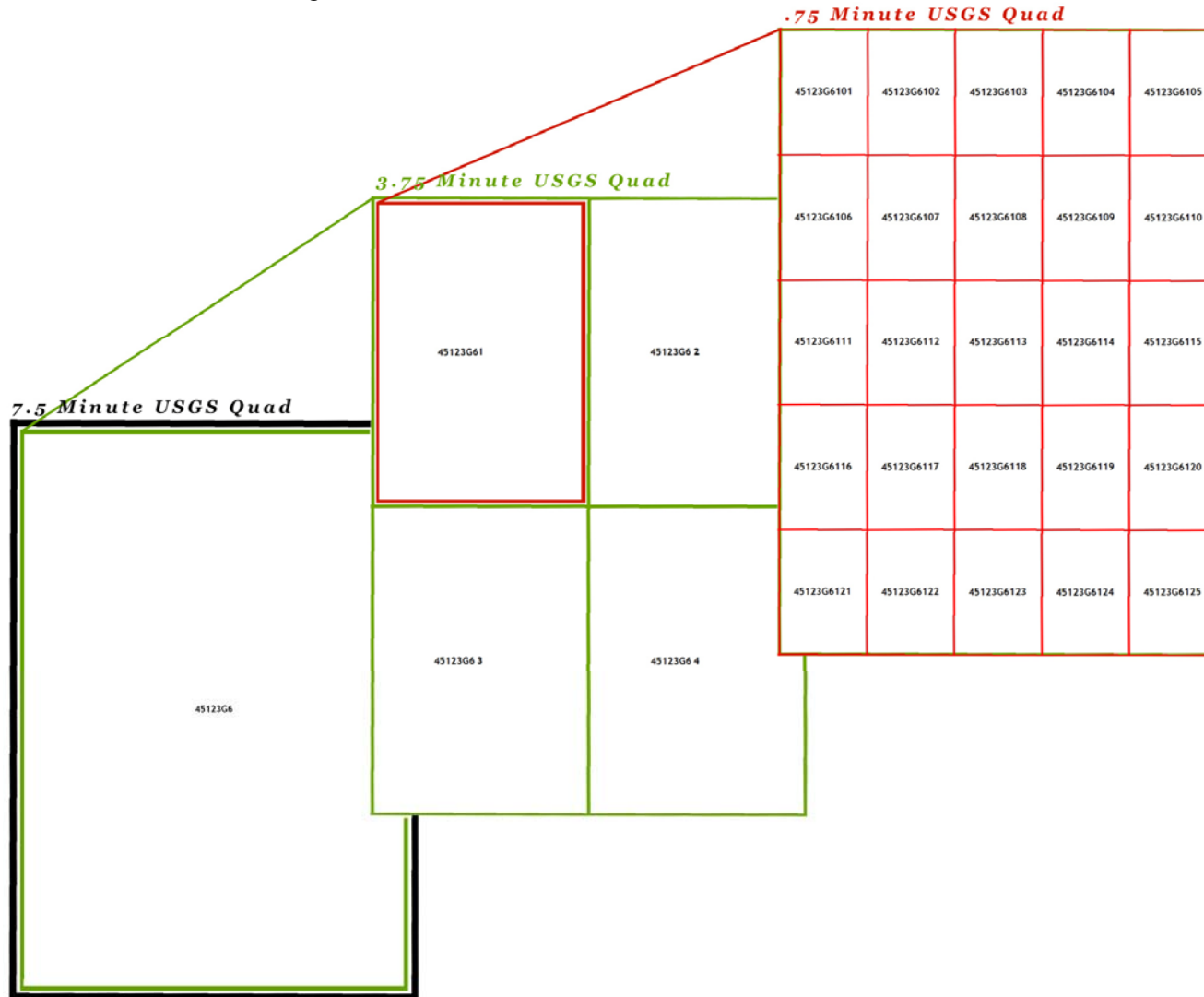
5.5 Datum and Projection

The data were processed as ellipsoidal elevations and required a Geoid transformation to be converted into orthometric elevations (NAVD88). In TerraScan, the NGS published Geiod03 model is applied to each point. The data were processed using meters in the Universal Transverse Mercator (UTM) Zone 10 and NAD83 (CORS96)/NAVD88 datum and converted to the respective projections for each data set as specified below.

- ODF AOIs are delivered in Oregon Lambert, EPSG 2992, with horizontal units in International Feet and vertical units in US Survey Feet, in the NAD83/NAVD88 datum (Geoid 03).

- All other AOIs are delivered in Oregon State Plane North, with horizontal units in International Feet and vertical units in US Survey Feet, in the NAD83 HARN/NAVD88 datum (Geoid 03).

6. Selected Images

6.1 Three Dimensional Oblique View Data Pairs

Example areas are presented to show paired, same-scene 3-D oblique view imagery (see **Figures 27-61**). These pairs depict a point cloud of all points colored by elevation and intensity shading (top image), and a 0.5-meter resolution triangulated irregular network (TIN) model of ground-classified LiDAR points colored by elevation (bottom image). Please note that the oblique view images are not north-oriented.

Figure 27. 3-d oblique view of LiDAR-derived surfaces in Quad 45123G6115, showing the North Fork Nehalem River and Hamlet Road in the ODF North Study Area (top image derived from all points, bottom image derived from ground-classified points).
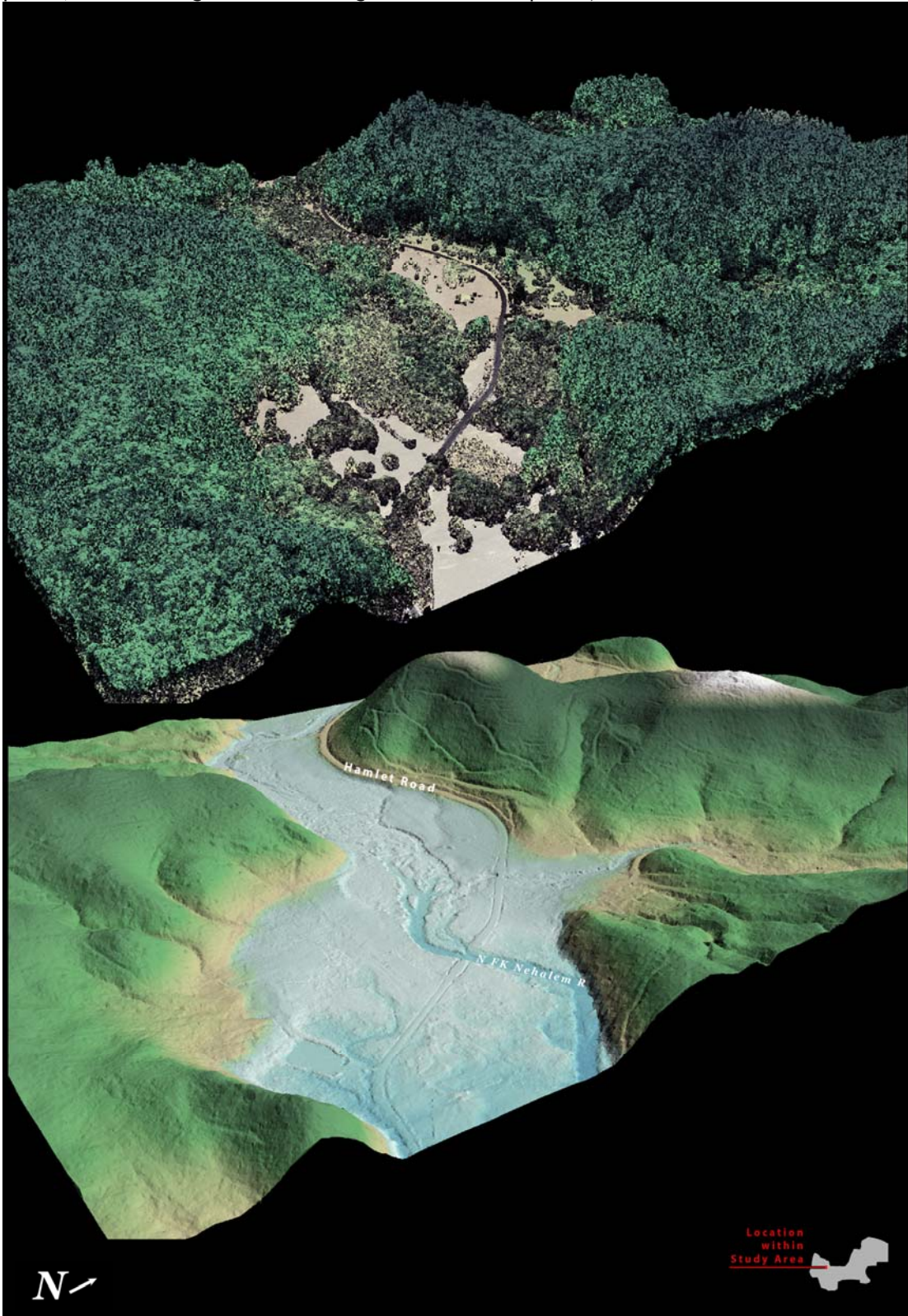
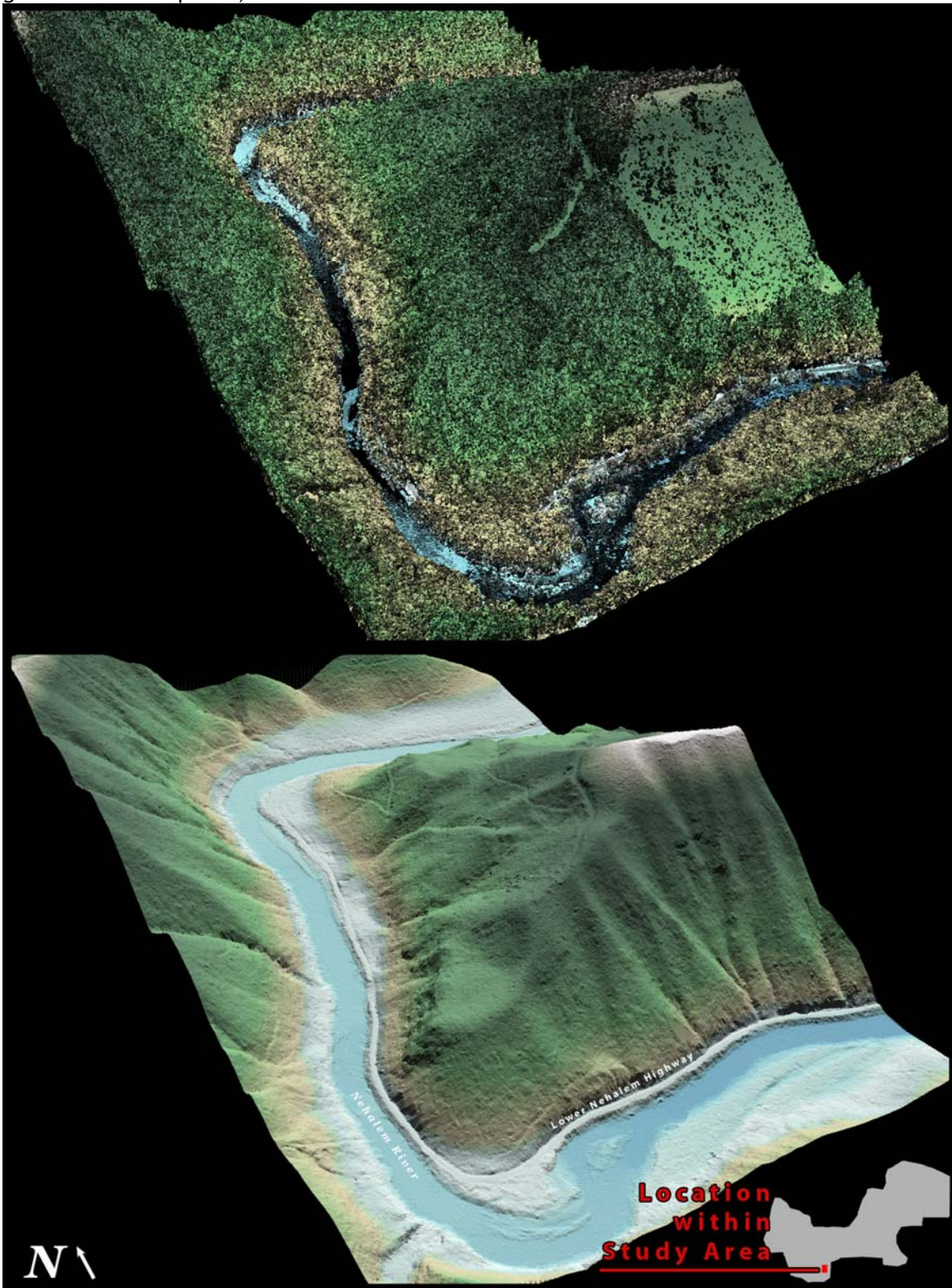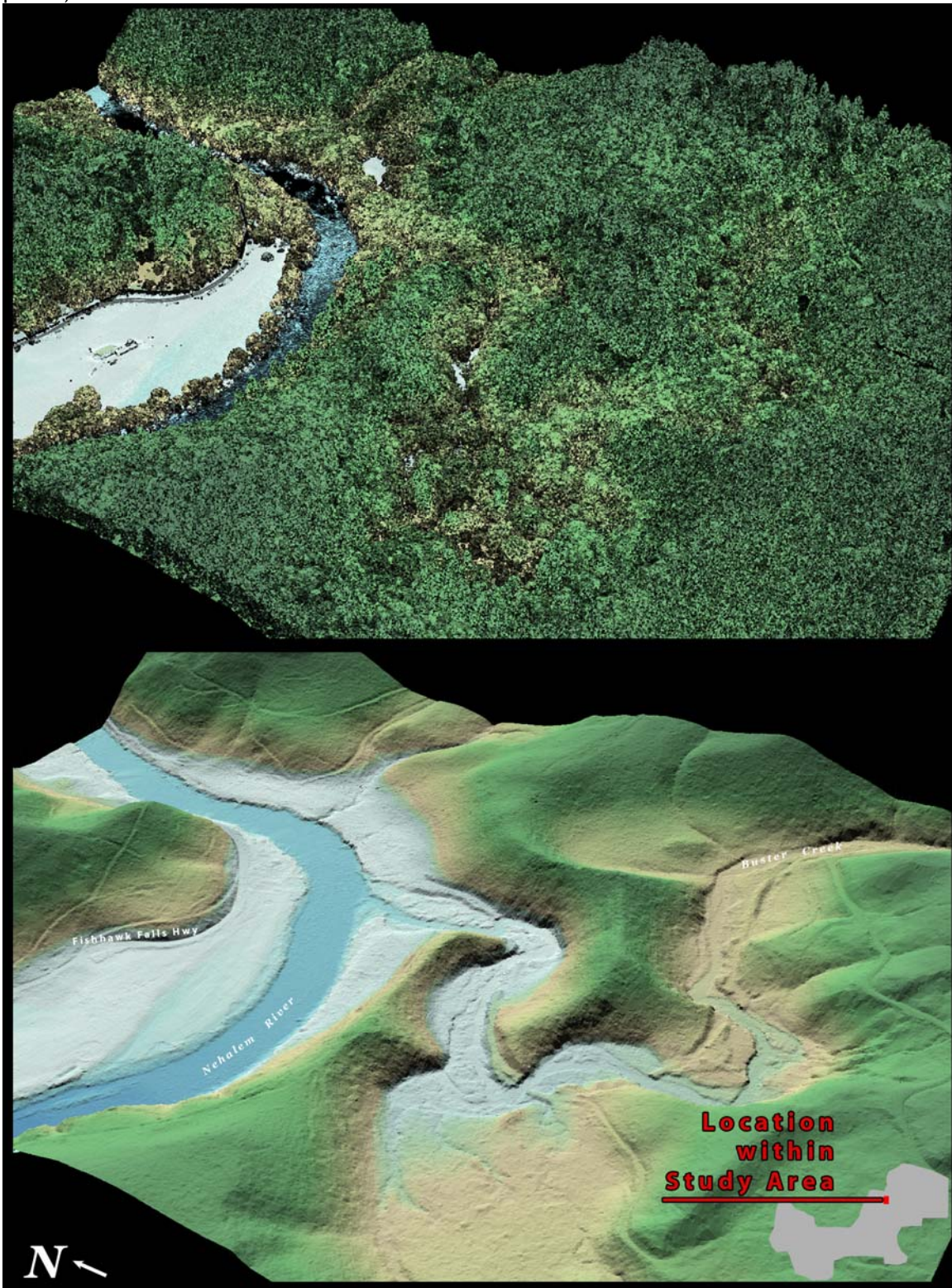**Figure 28.** 3-d oblique view of LiDAR-derived surfaces in Quad 45123G6414, showing the Nehalem River and the Lower Nehalem Highway, just inside the Clatsop State Forest boundary in the ODF North Study Area. (Top image derived from all points, bottom image derived from ground-classified points).

Figure 29. 3-d oblique view of LiDAR-derived surfaces in Quad 45123G6414, showing the confluence of Buster Creek with the Nehalem River, and Fishhawk Falls Road in the ODF North Study Area. (Top image derived from all points, bottom image derived from ground-classified points).

Figure 30. 3-d oblique view of LiDAR-derived surfaces in 0.75' Quad 45122A7223-224,403-404, showing the Mount Angel Abbey in the DOGAMI study area (top image derived from all points, bottom image derived from ground-classified points).
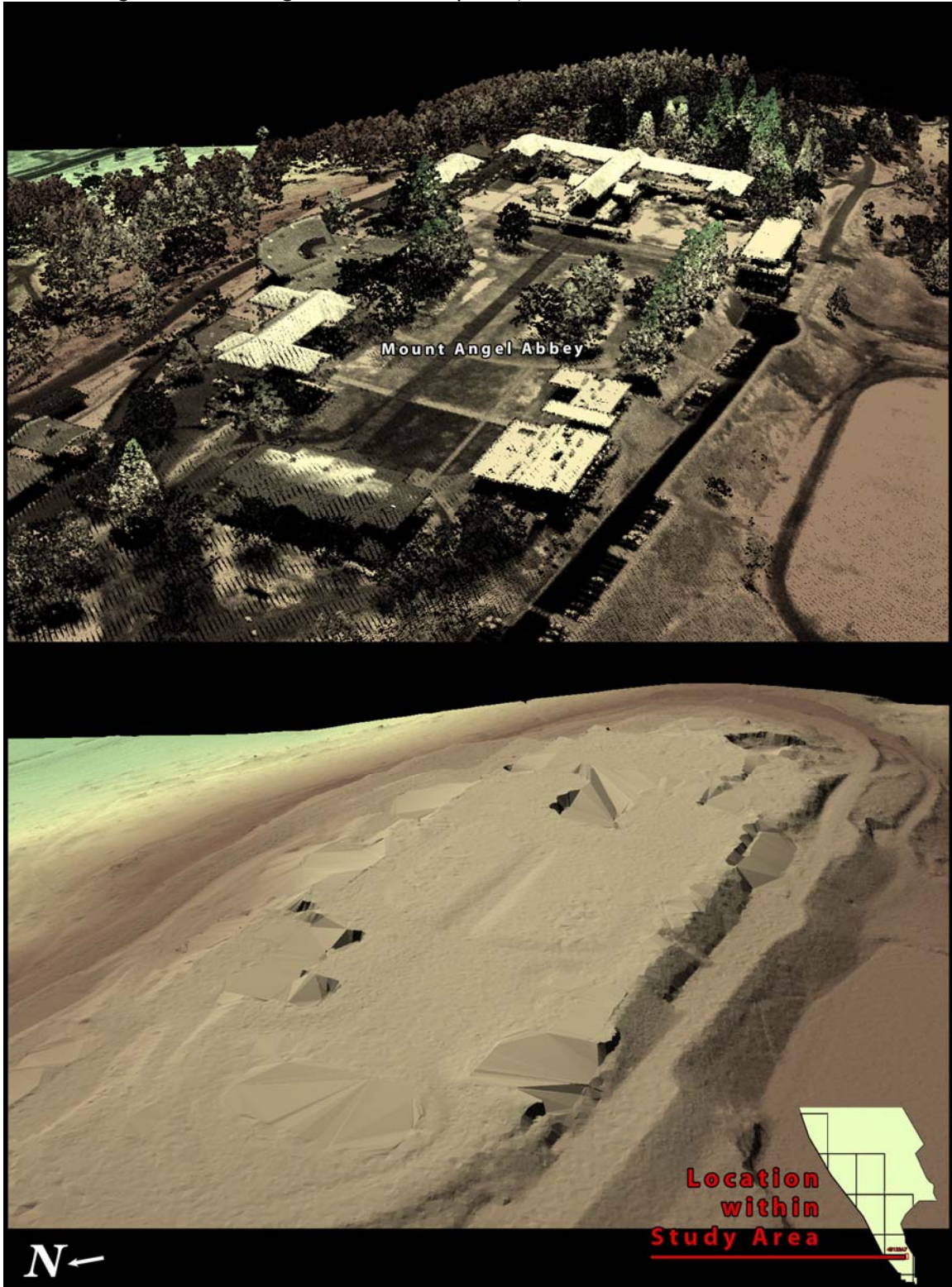
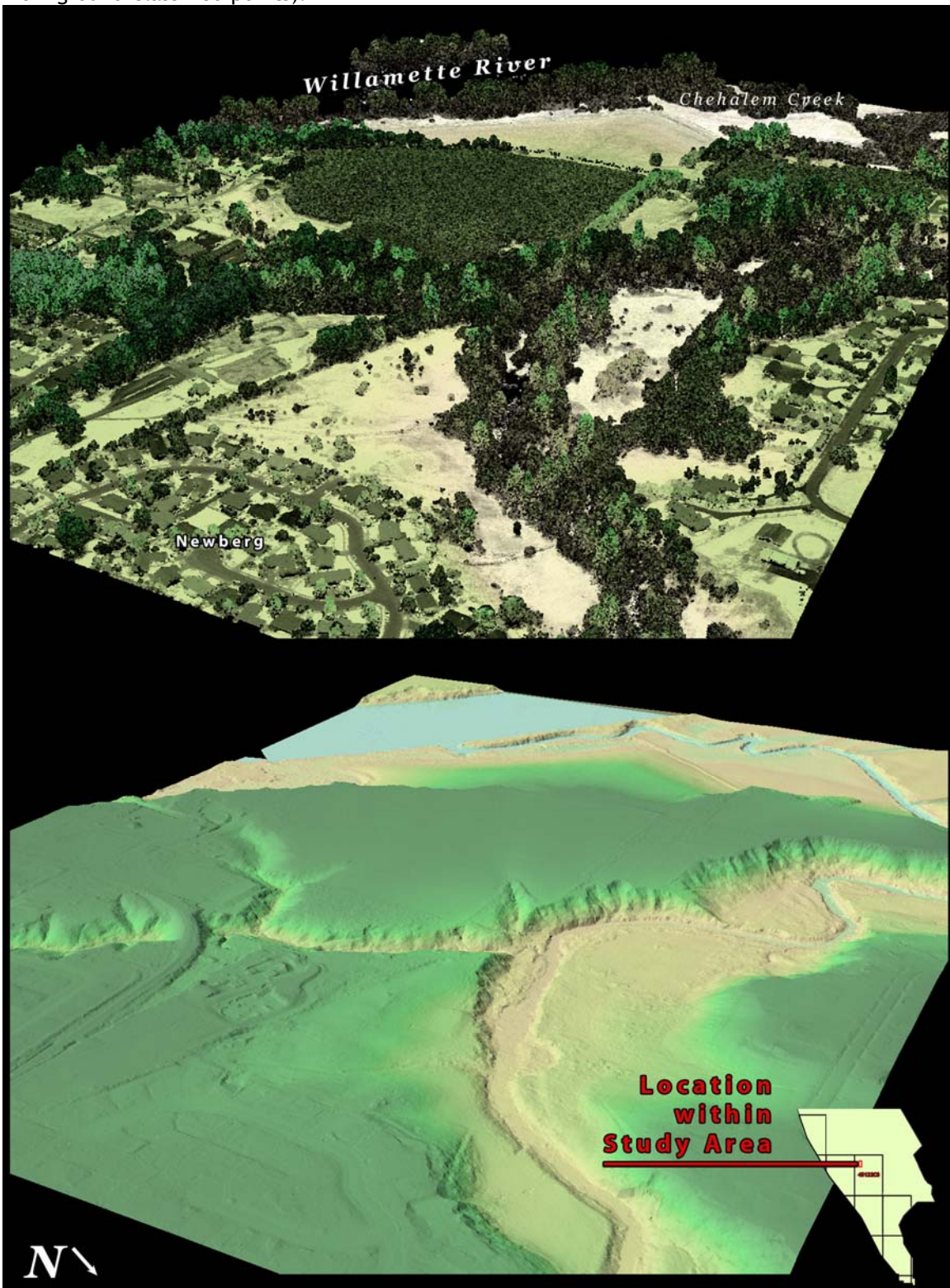**Figure 31.** 3-d oblique view of LiDAR-derived surfaces in 0.75' Quad 45122A7108, showing a short reach of the Pudding River in the DOGAMI study area (top image derived from all points, bottom image derived from ground-classified points).
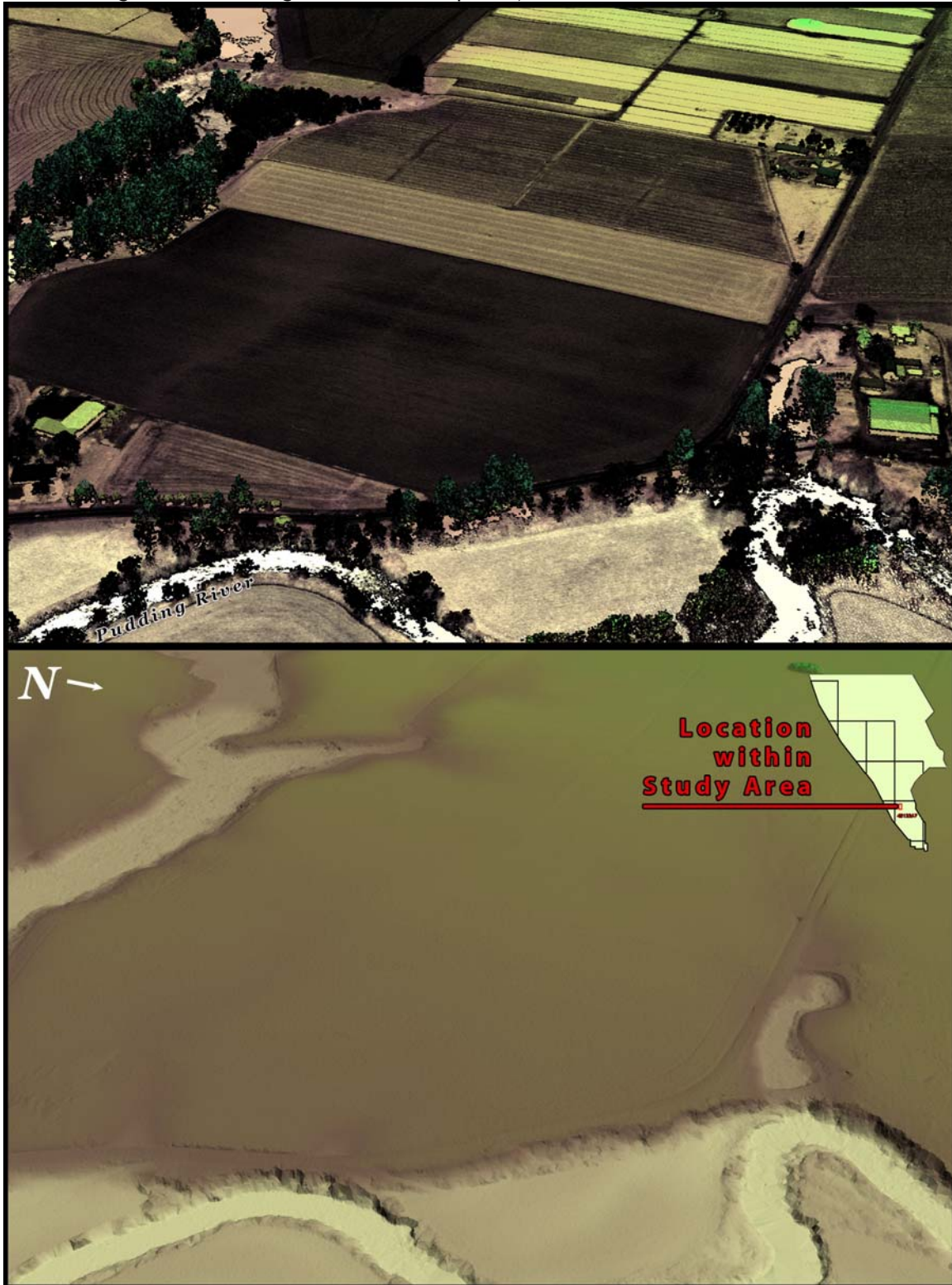
Figure 32. 3-d oblique view of LiDAR-derived surfaces in 0.75' Quad 45122C8307-308,312-313, showing the confluence of Chehalem Creek and the Willamette River, near the southwest edge of Newberg in the DOGAMI study area (top image derived from all points, bottom image derived from ground-classified points).

LiDAR Remote Sensing Data: Department of Geology and Mineral Industries and Oregon Department of Forestry
Prepared by Watershed Sciences, Inc.   *February 19, 2008*

Figure 33. 3-d oblique view of LiDAR-derived surfaces in 0.75' Quad 45123D2109-110,114-115, showing Henry Hagg Lake and Scoggins Creek in the DOGAMI study area (top image derived from all points, bottom image derived from ground-classified points).
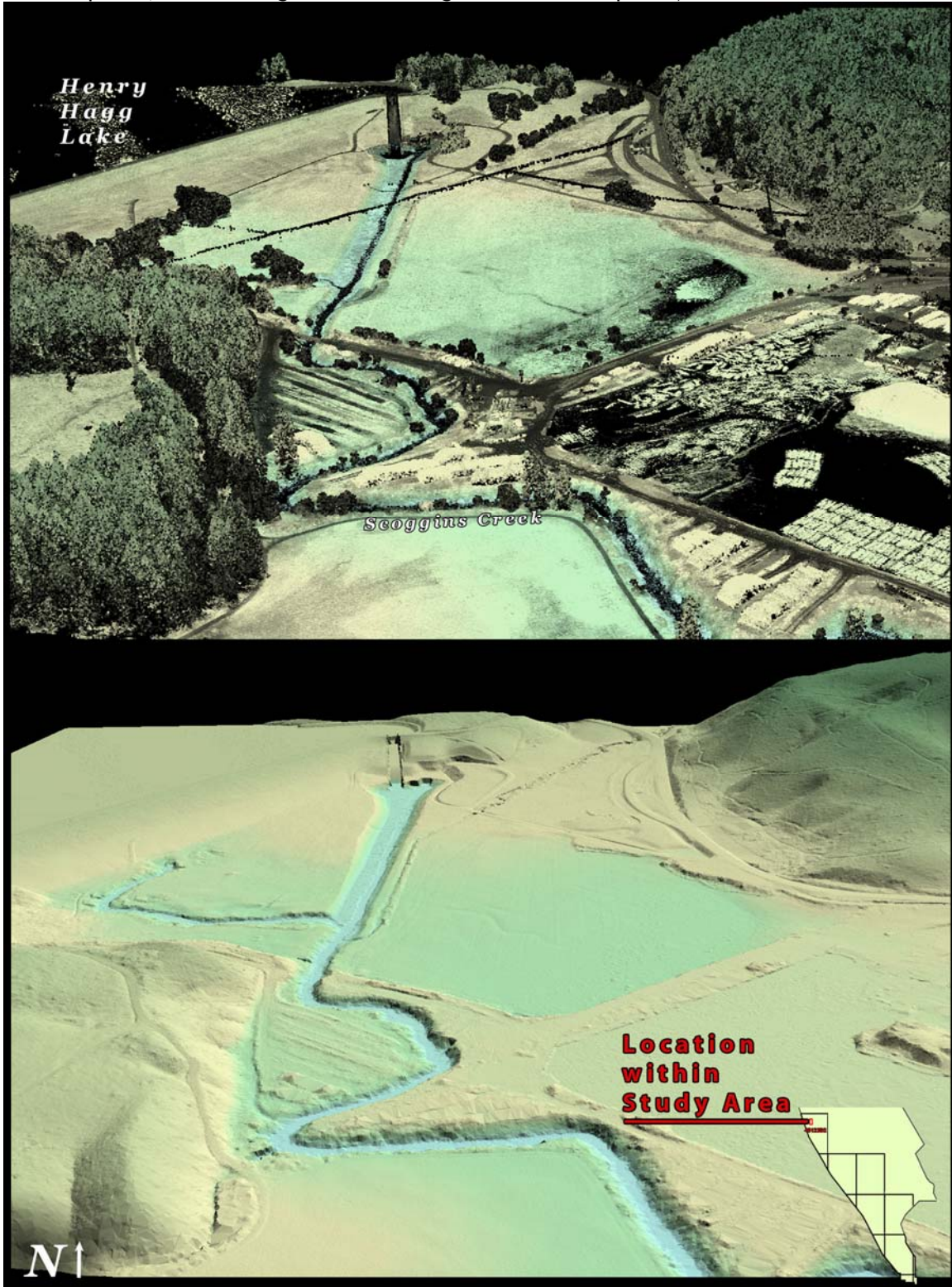
Figure 34. 3-d oblique view of LiDAR-derived surfaces in 7.5' Quad 45123D7, showing Kilchis and Wilson Rivers in the ODF South study area.
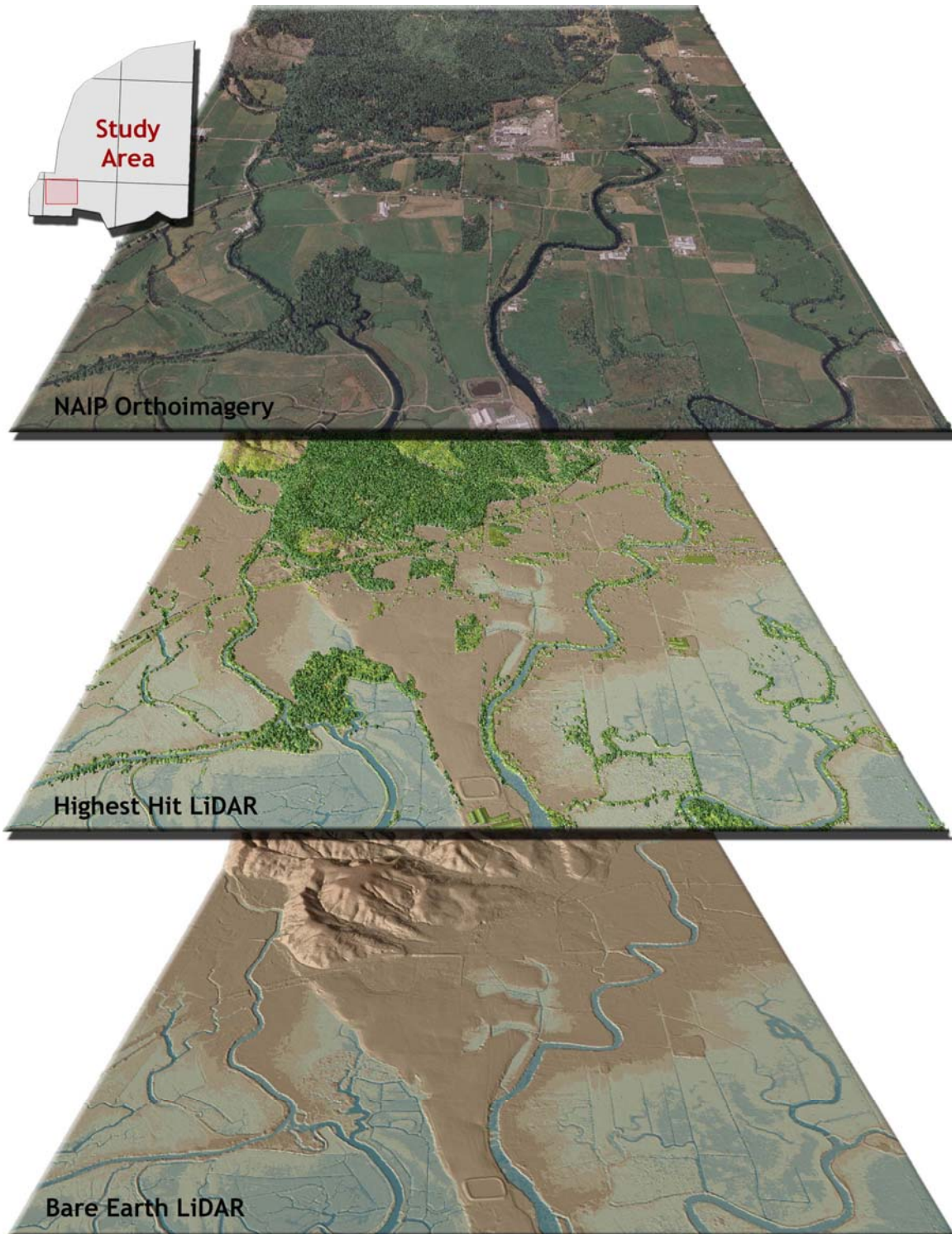
Figure 35. 3-d oblique view of LiDAR-derived surfaces in 7.5' Quad 45123D6, showing Wilson River near the Little North Fork confluence in the ODF South study area.
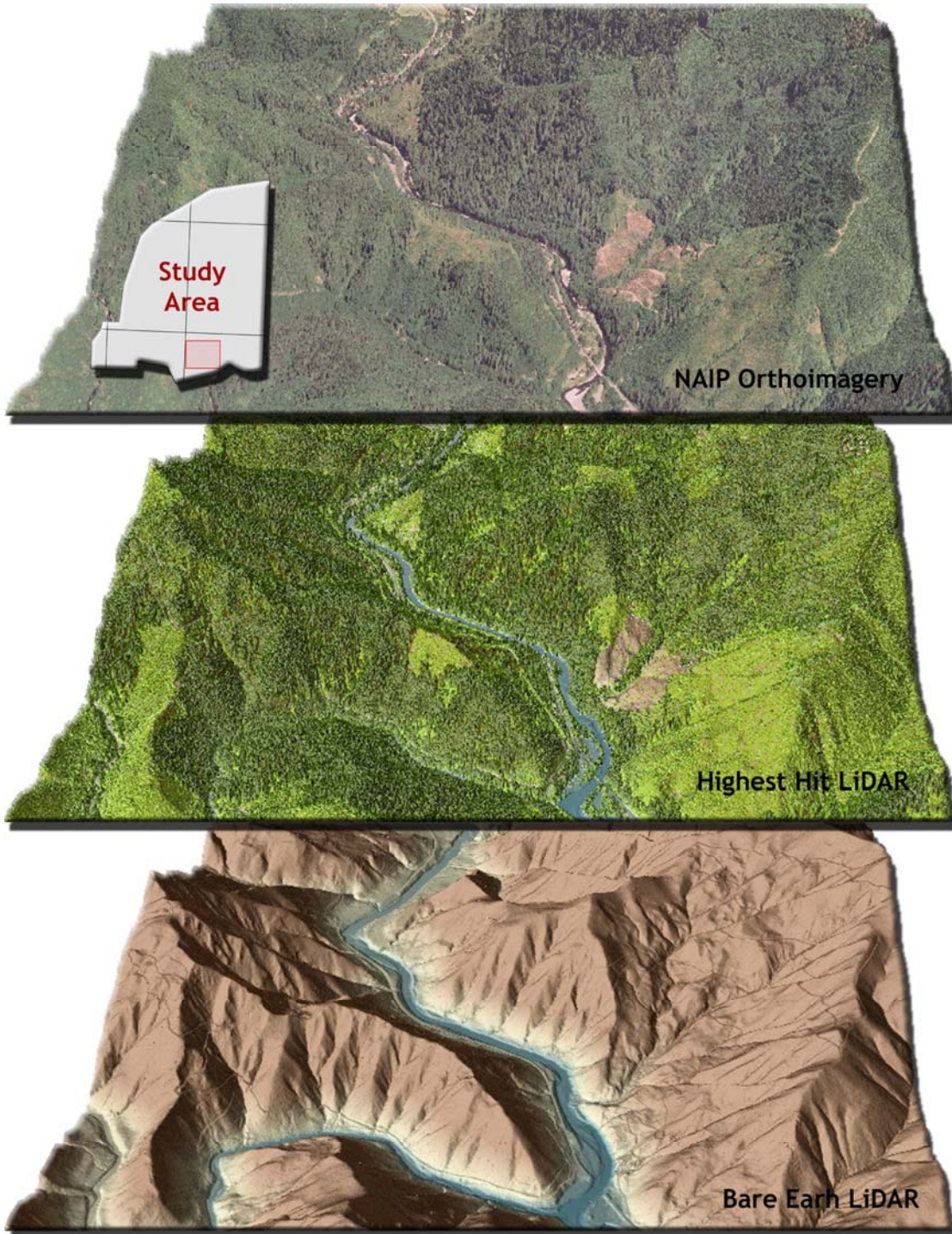
45

LiDAR Remote Sensing Data: Department of Geology and Mineral Industries and Oregon Department of Forestry
Prepared by Watershed Sciences, Inc. *February 19, 2008*

Figure 36. 3-d oblique view of LiDAR-derived surfaces in 7.5' Quad 45123D6, showing the confluence of the Wilson and Little North Fork Rivers in the ODF South study area.
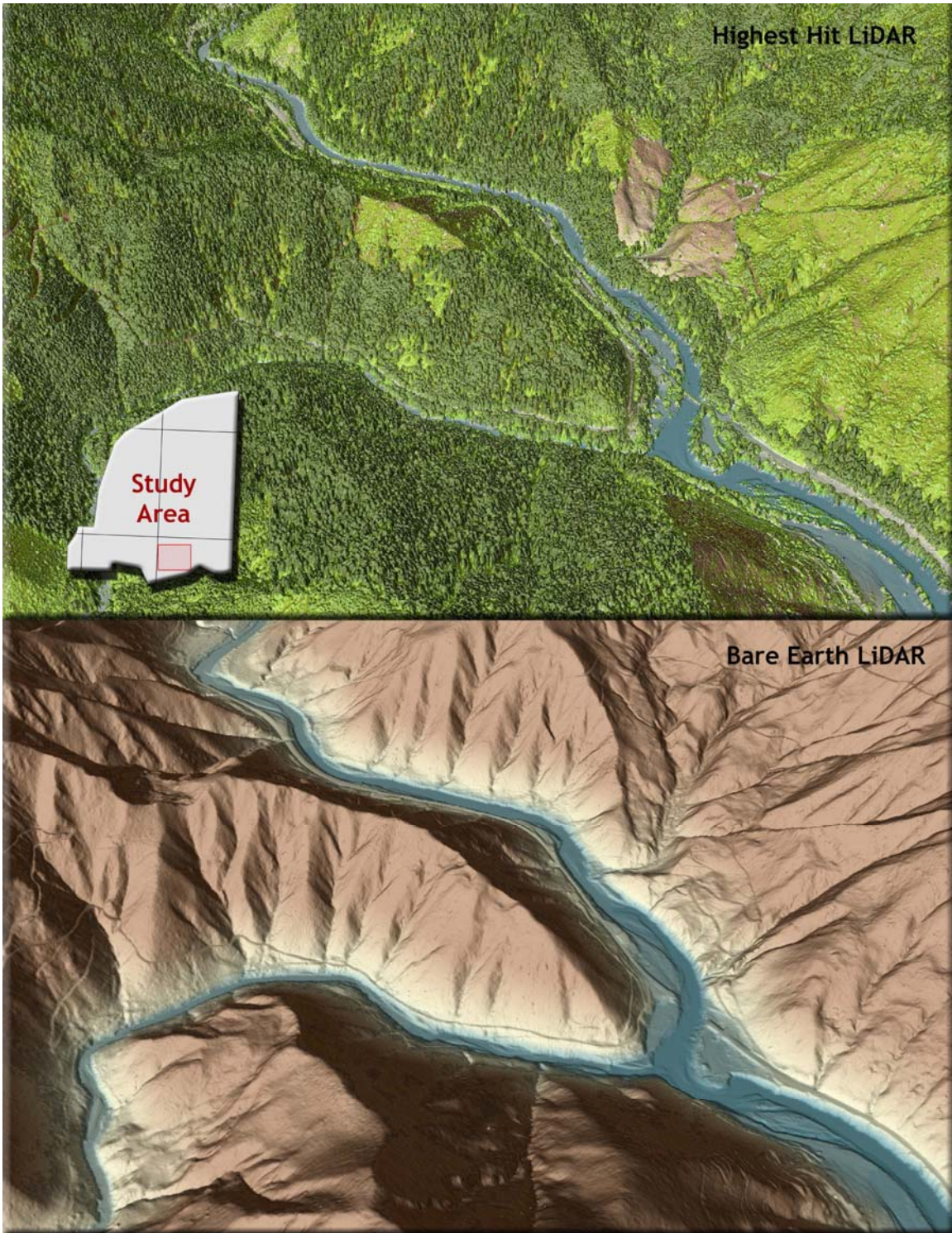
Figure 37. 3-d oblique view of LiDAR-derived surfaces in 7.5' Quad 45123E6, showing the upper portion of the Little North Fork Wilson River watershed in the ODF South study area.

LiDAR Remote Sensing Data: Department of Geology and Mineral Industries and Oregon Department of Forestry
Prepared by Watershed Sciences, Inc.   *February 19, 2008*

Figure 38. 3-d oblique view of LiDAR-derived surfaces showing a view of the Devils Lake Fork upper watershed.
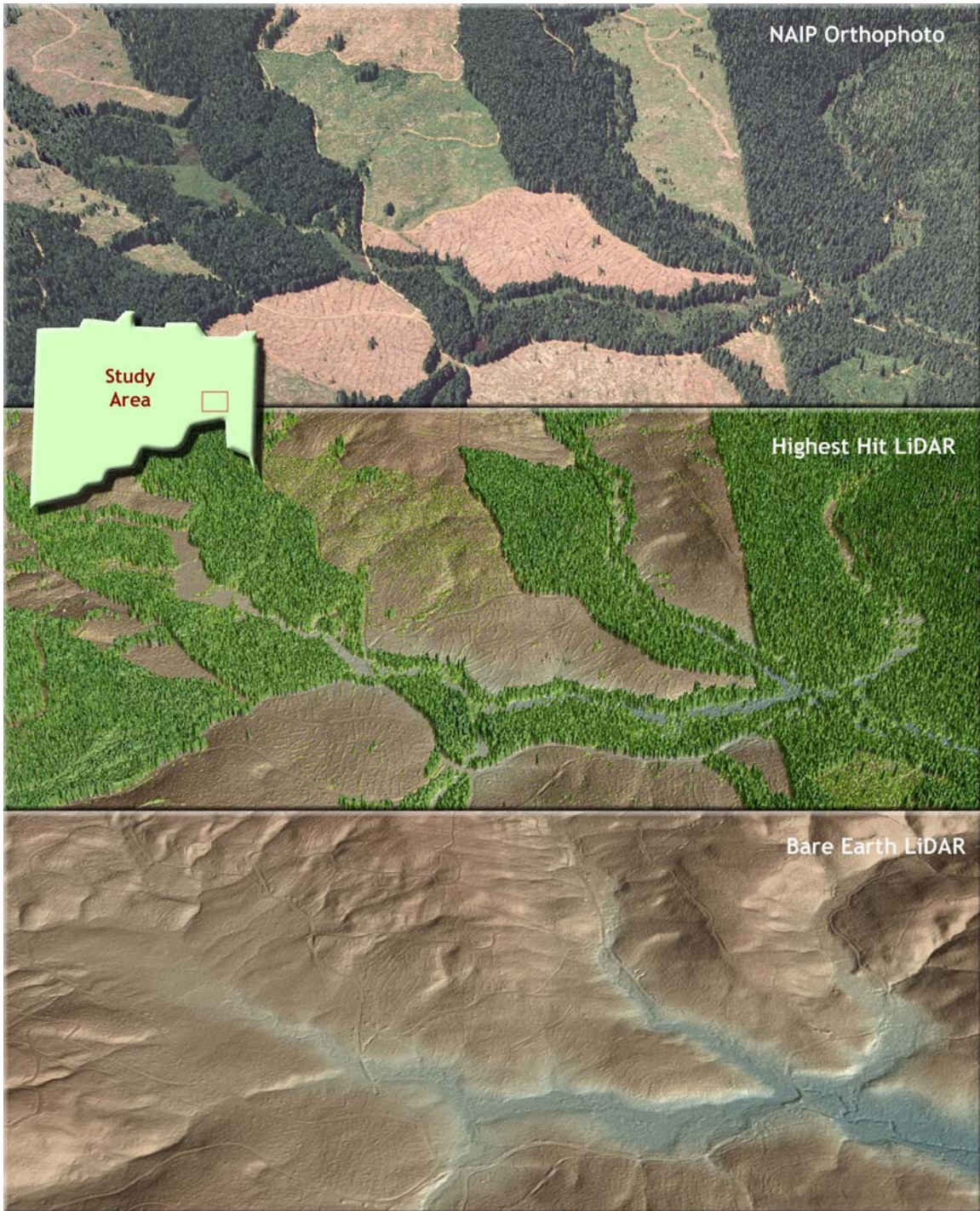
Figure 39. 3-d oblique view of LiDAR-derived surfaces looking south over the Wilson River near the North Fork confluence.

Figure 40. 3-d oblique view of LiDAR-derived surfaces looking south over the Wilson River near the North Fork confluence.
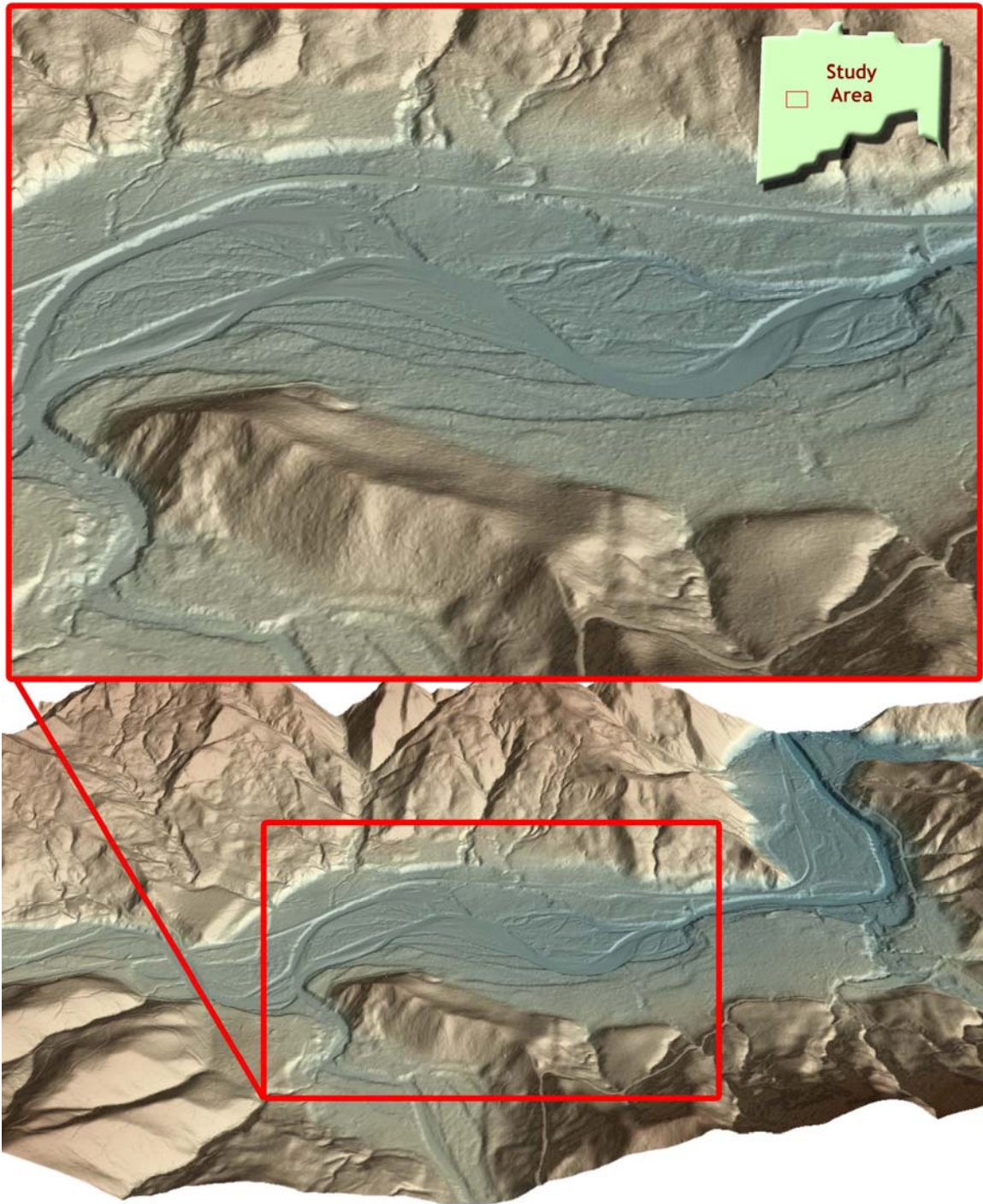
LiDAR Remote Sensing Data: Department of Geology and Mineral Industries and Oregon Department of Forestry
Prepared by Watershed Sciences, Inc.   *February 19, 2008*

Figure 41. 3-d oblique view of LiDAR-derived surfaces showing an historic landslide along Devils Lake Fork, between Elliot Creek and Drift Creek.

Figure 42. 3-d oblique view of LiDAR-derived surfaces looking north across confluence of Gales Creek and Beaver Creek.
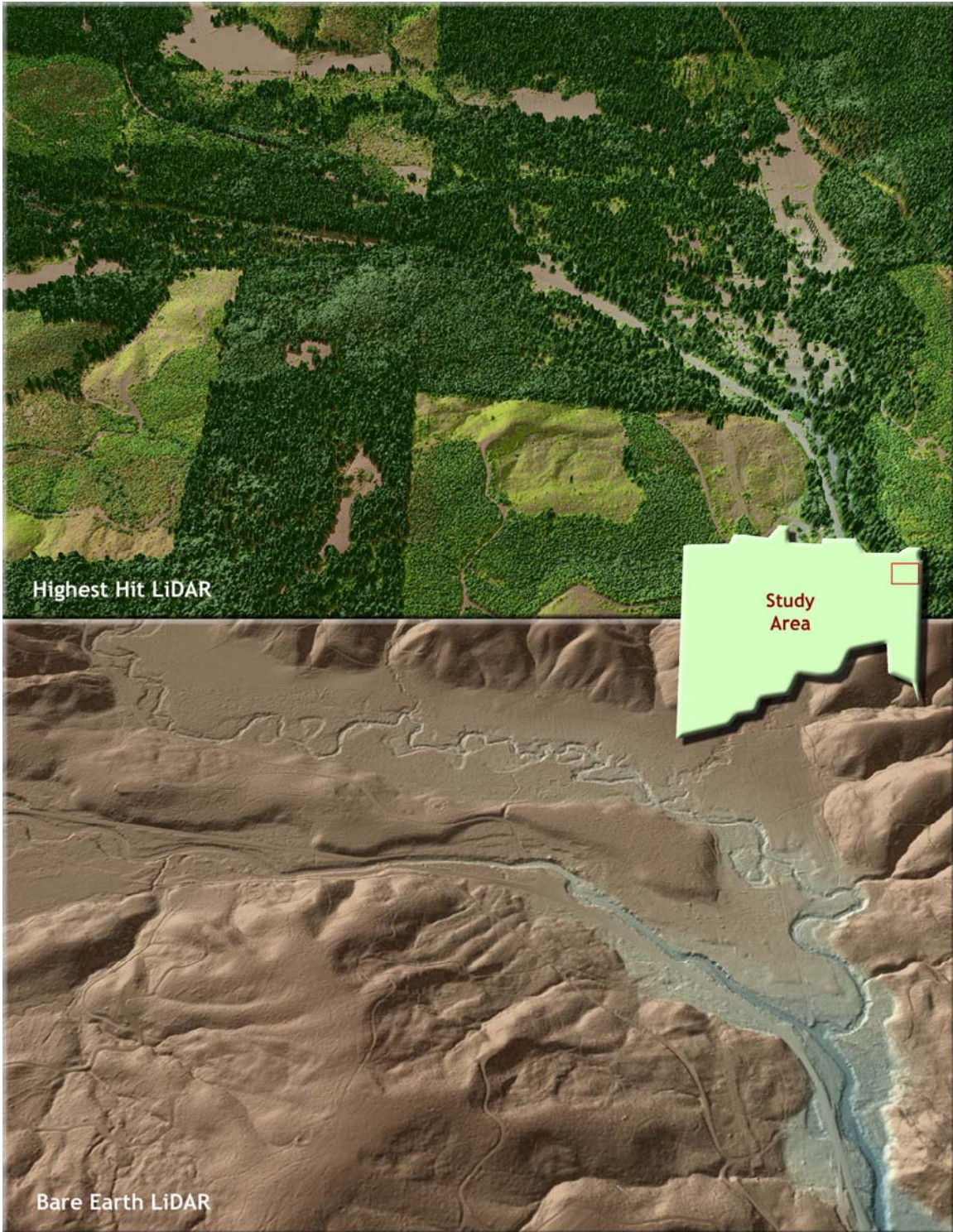

Highest Hit LiDAR

Study Area

Bare Earth LiDAR

Figure 43. 3-d oblique view of LiDAR-derived surfaces showing the Wilson River at the Jordan Creek confluence.
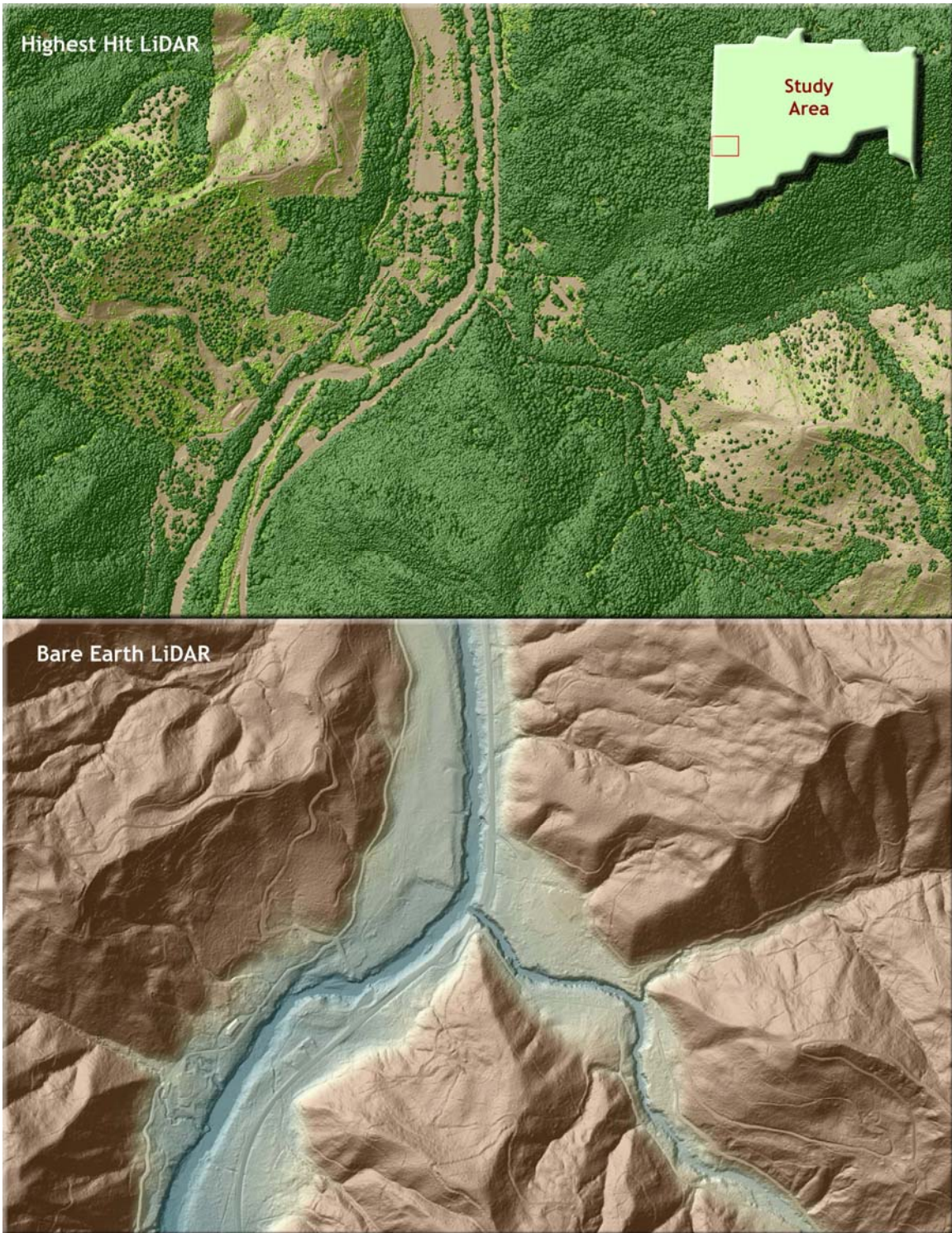
Figure 44. 3-d oblique view of LiDAR-derived surfaces showing an historic landslide along Wolf Creek.
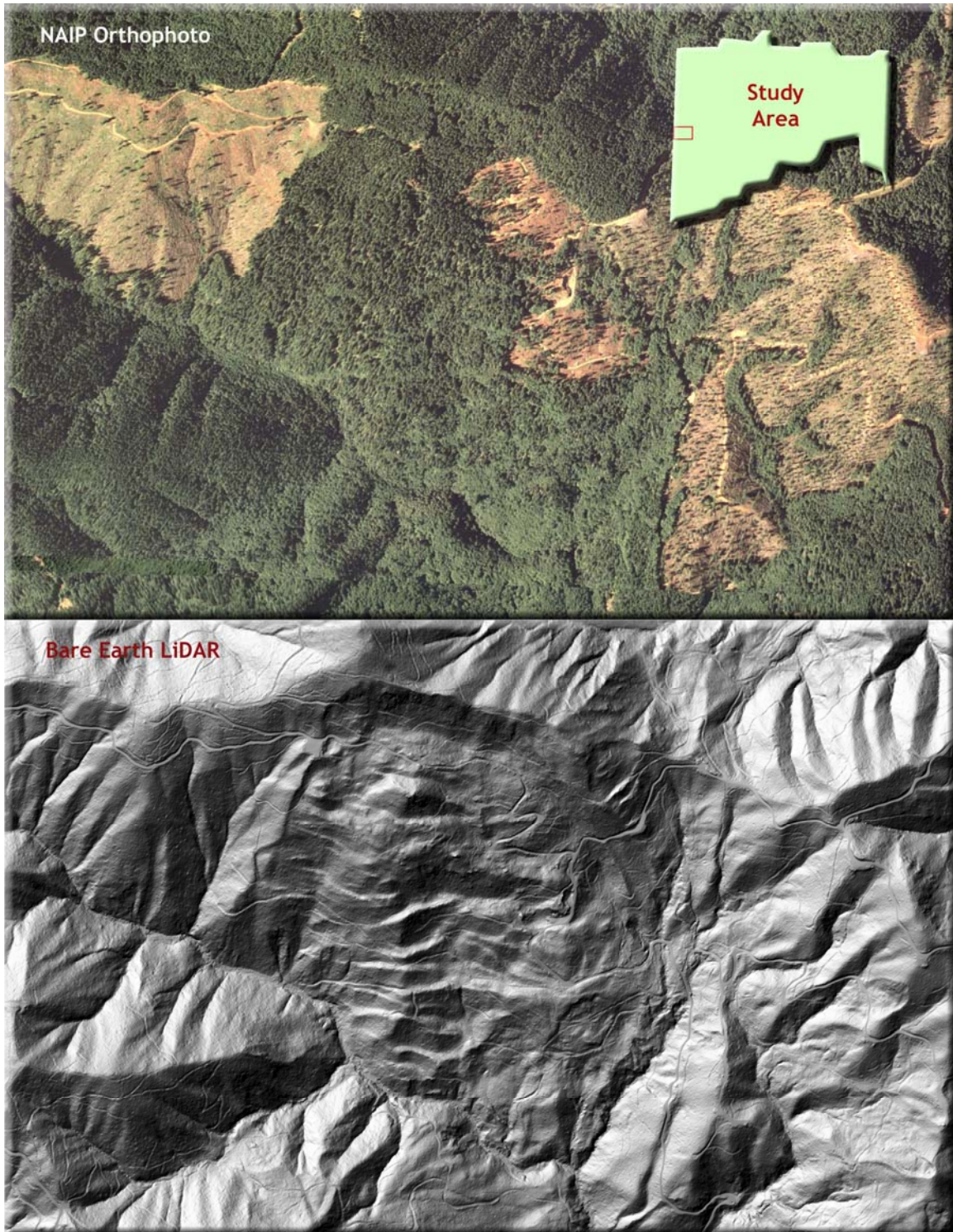
Figure 45. 3-d oblique view of LiDAR-derived images showing the highest hit surface of downtown Portland, looking eastward.
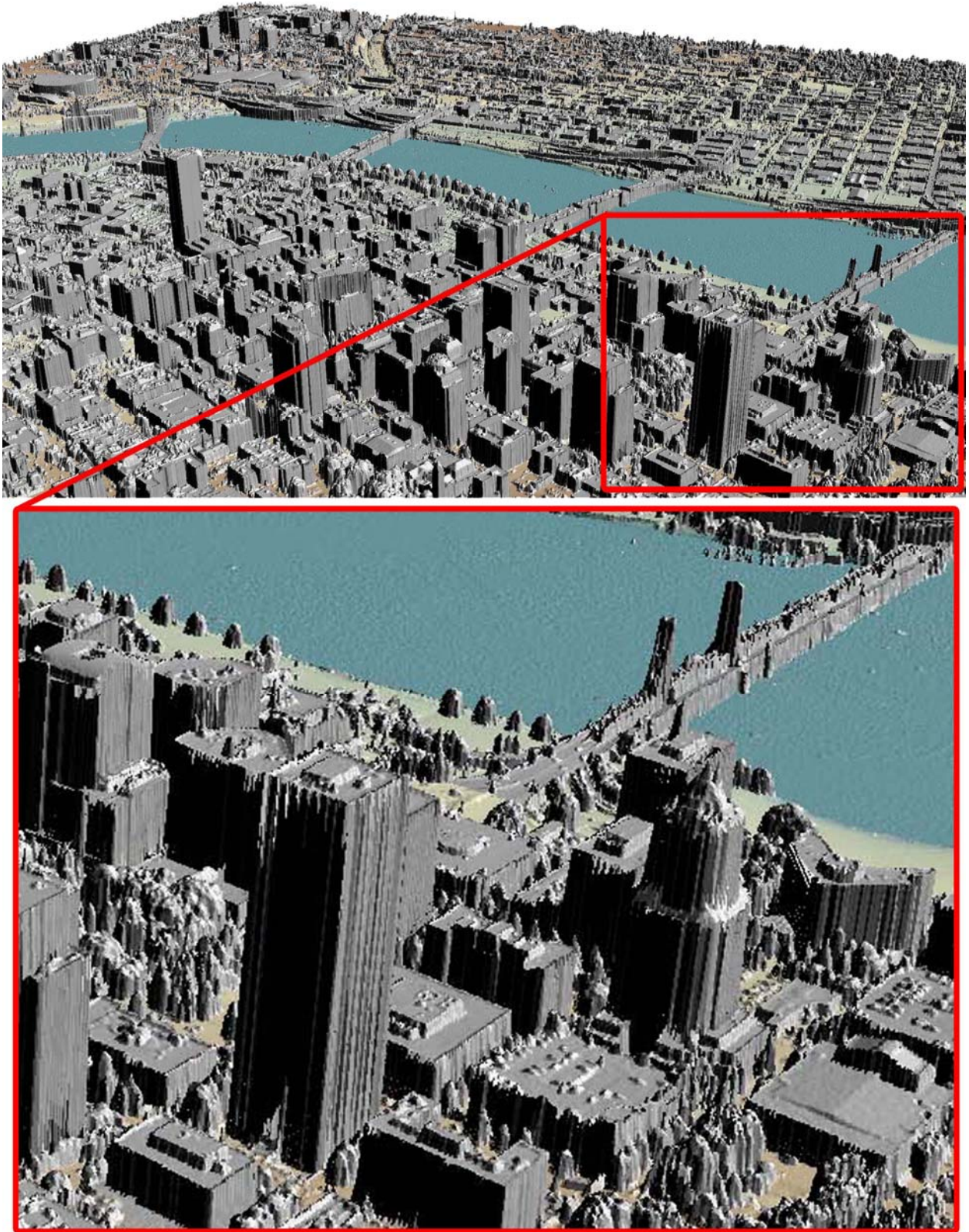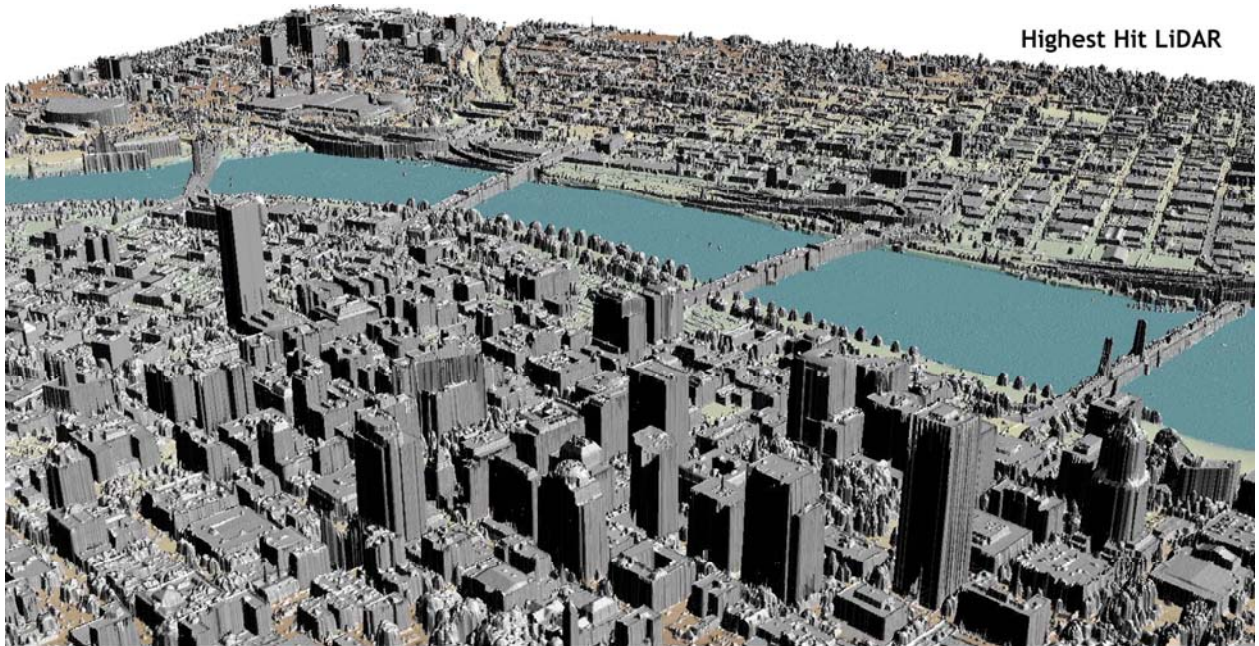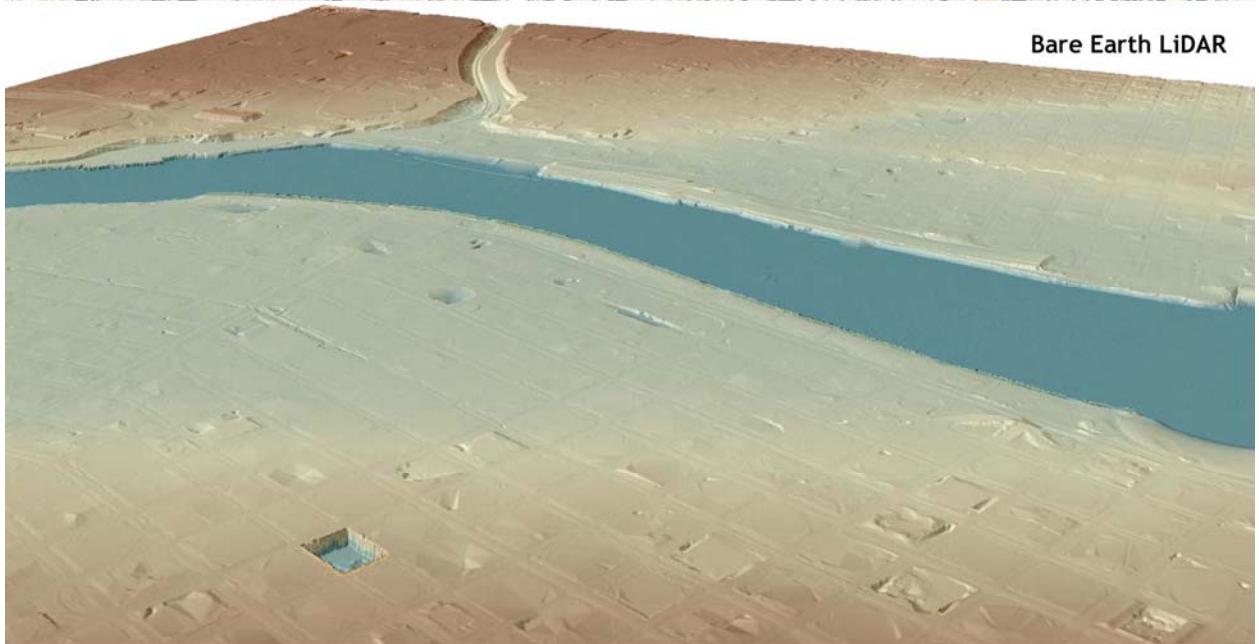
Figure 46. 3-d oblique view of LiDAR-derived surfaces showing the city of Portland, looking eastward.

Highest Hit LiDAR

Bare Earth LiDAR

Figure 47. 3-d oblique view of downtown Portland, looking westward. Bottom image is of LiDAR-derived highest hit surface.
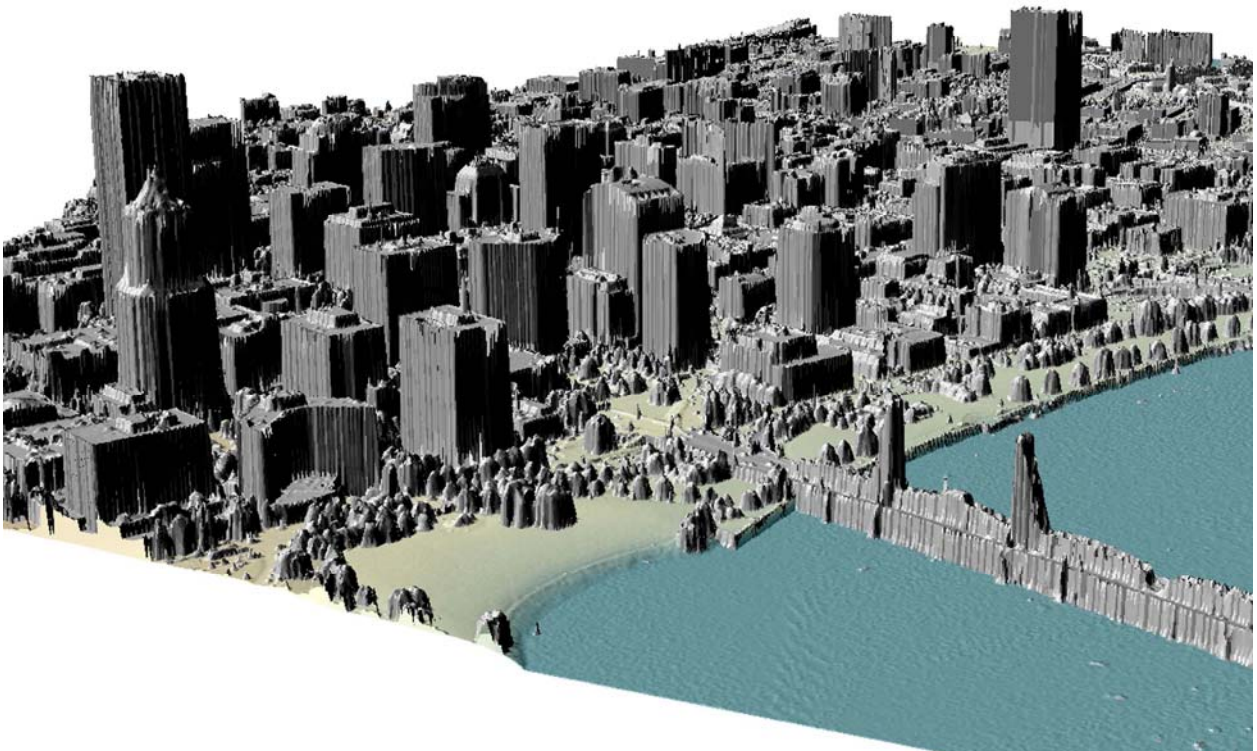
Figure 48. 3-d oblique view of Ladd's Addition in Southeast Portland.

Figure 49. 3-d oblique view North Willamette Boulevard, just east of the University of Portland.

NAIP Orthophoto

Highest Hit LiDAR

Bare Earth LiDAR

LiDAR Remote Sensing Data: Department of Geology and Mineral Industries and Oregon Department of Forestry
Prepared by Watershed Sciences, Inc.   *February 19, 2008*

Figure 50. 3-d oblique view of the I-5 and I-84 interchange near downtown Portland.
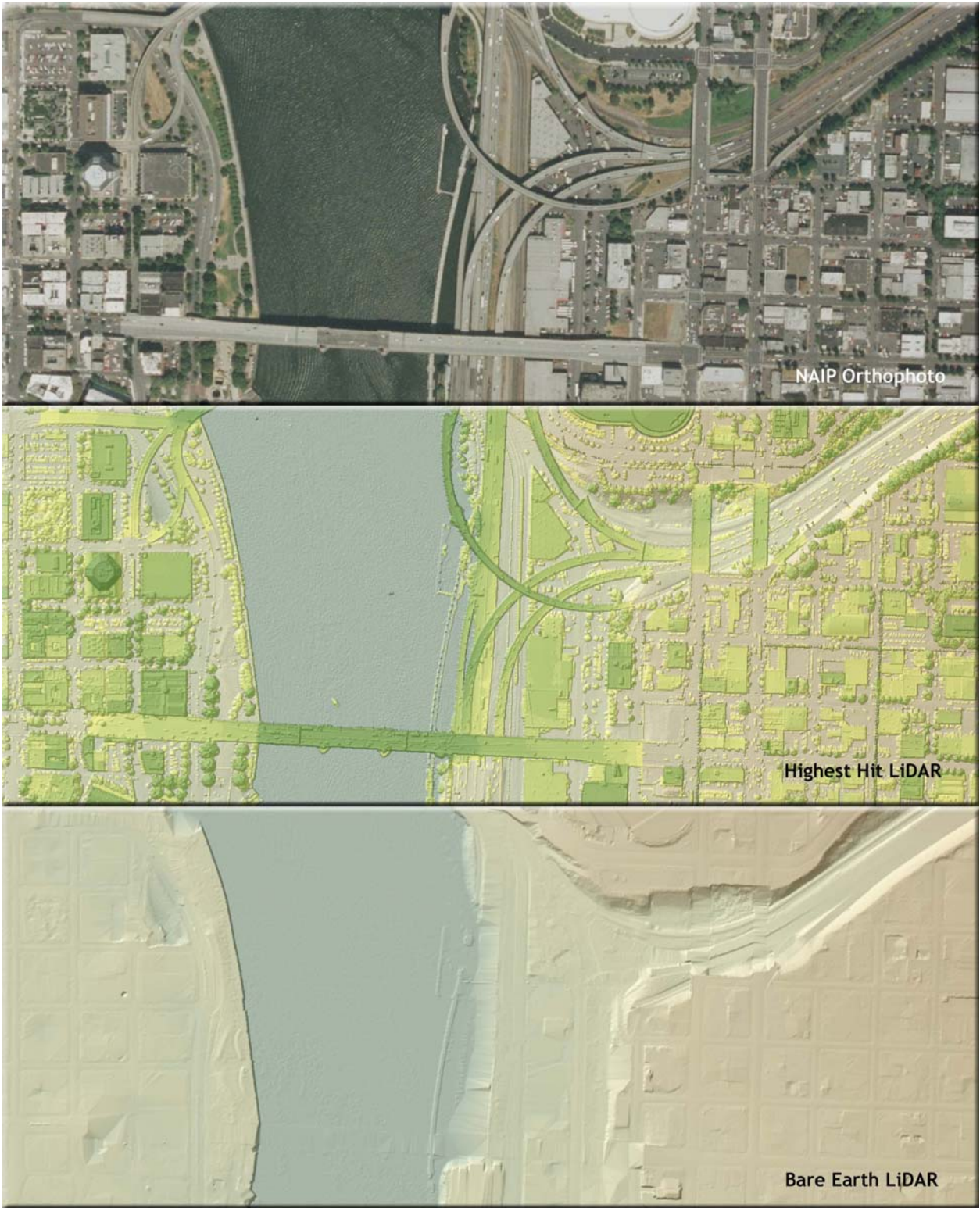
Figure 51. 3-d oblique view Looking southward at Willamette National Cemetery and nearby residential development.

Figure 52. 3-d oblique view of the Clackamas River, just downstream of Carver, OR (looking southward).

Figure 53. 3-d oblique view looking southward at Walters Hill and Johnson Creek in Gresham.
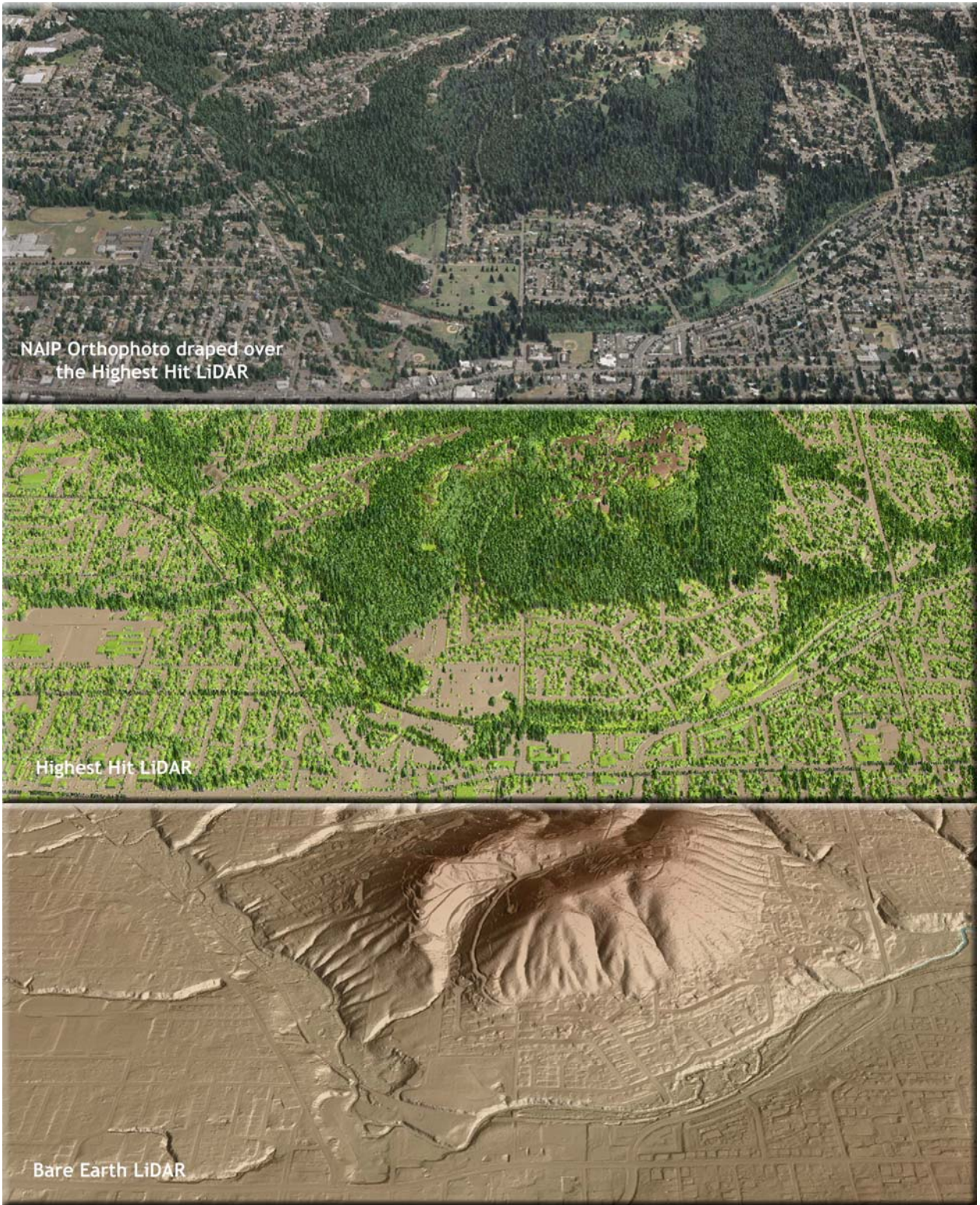
Figure 54. 3-d oblique view looking northward at Clear Creek near Redland.

Highest Hit LiDAR

Bare Earth LiDAR

Figure 55. 3-d oblique view of the Clackamas River (looking upstream) near Foster Creek (entering from lower right of image) and Deep Creek (entering from upper left of image).
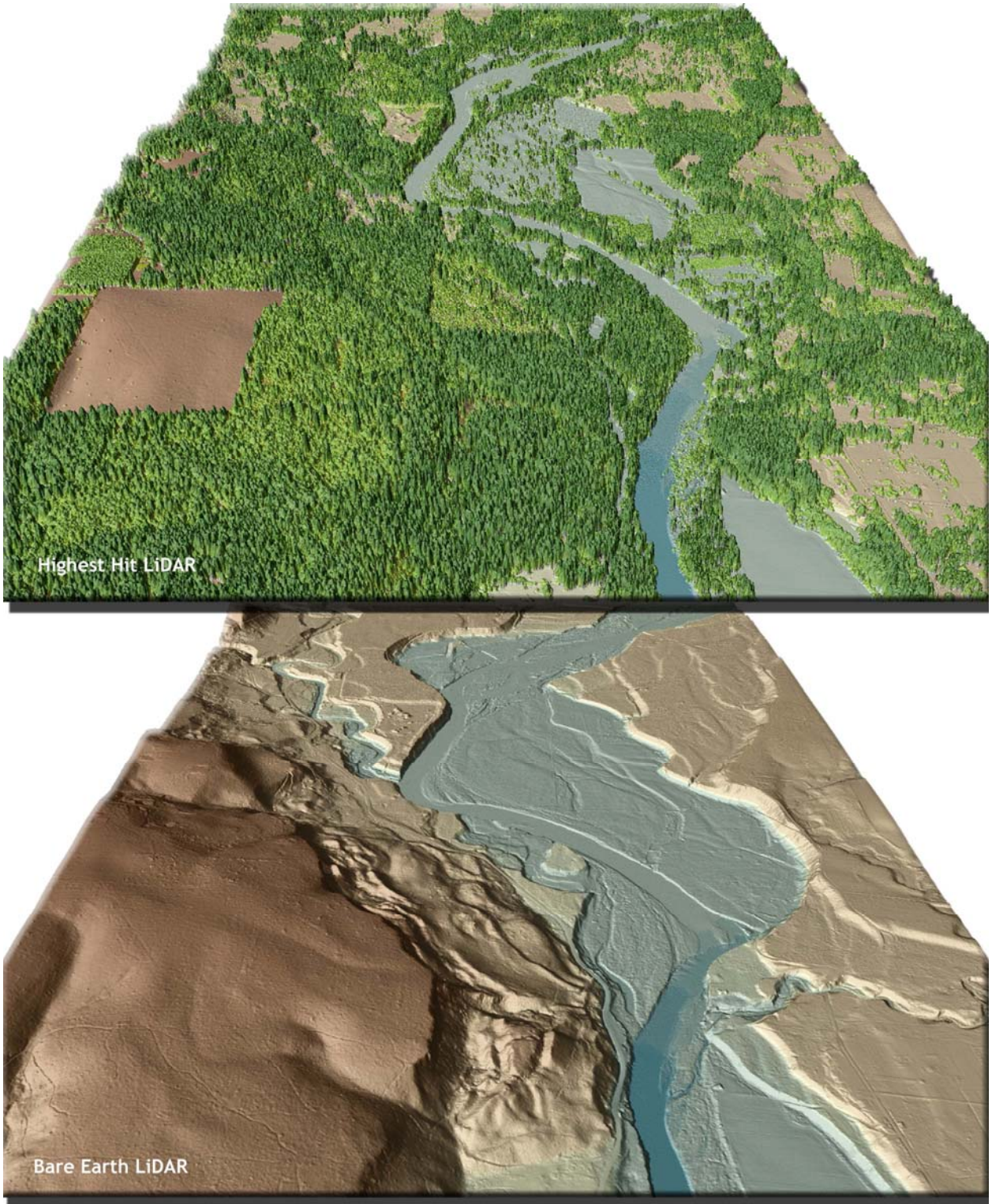

Highest Hit LiDAR

Bare Earth LiDAR

Figure 56. 3-d oblique view looking northward at Clackamas River at the Deep Creek confluence.

Figure 57. 3-d oblique view looking northward of Martin Creek (flows from bottom of image to upper left) and Mosier Creek (flows from bottom of image to upper right). The ridge between the creeks is The Hogback.

Figure 58. 3-d oblique view of the residential development in Northern Clackamas County near Borges Road.

NAIP Orthophoto draped over the Highest Hit LiDAR

Highest Hit LiDAR

Bare Earth LiDAR

Figure 59. 3-d oblique view looking northward at the ridge between Noyer Creek (left) and North Fork Deep Creek (right), near Barton.

LiDAR Remote Sensing Data: Department of Geology and Mineral Industries and Oregon Department of Forestry
Prepared by Watershed Sciences, Inc.   *February 19, 2008*
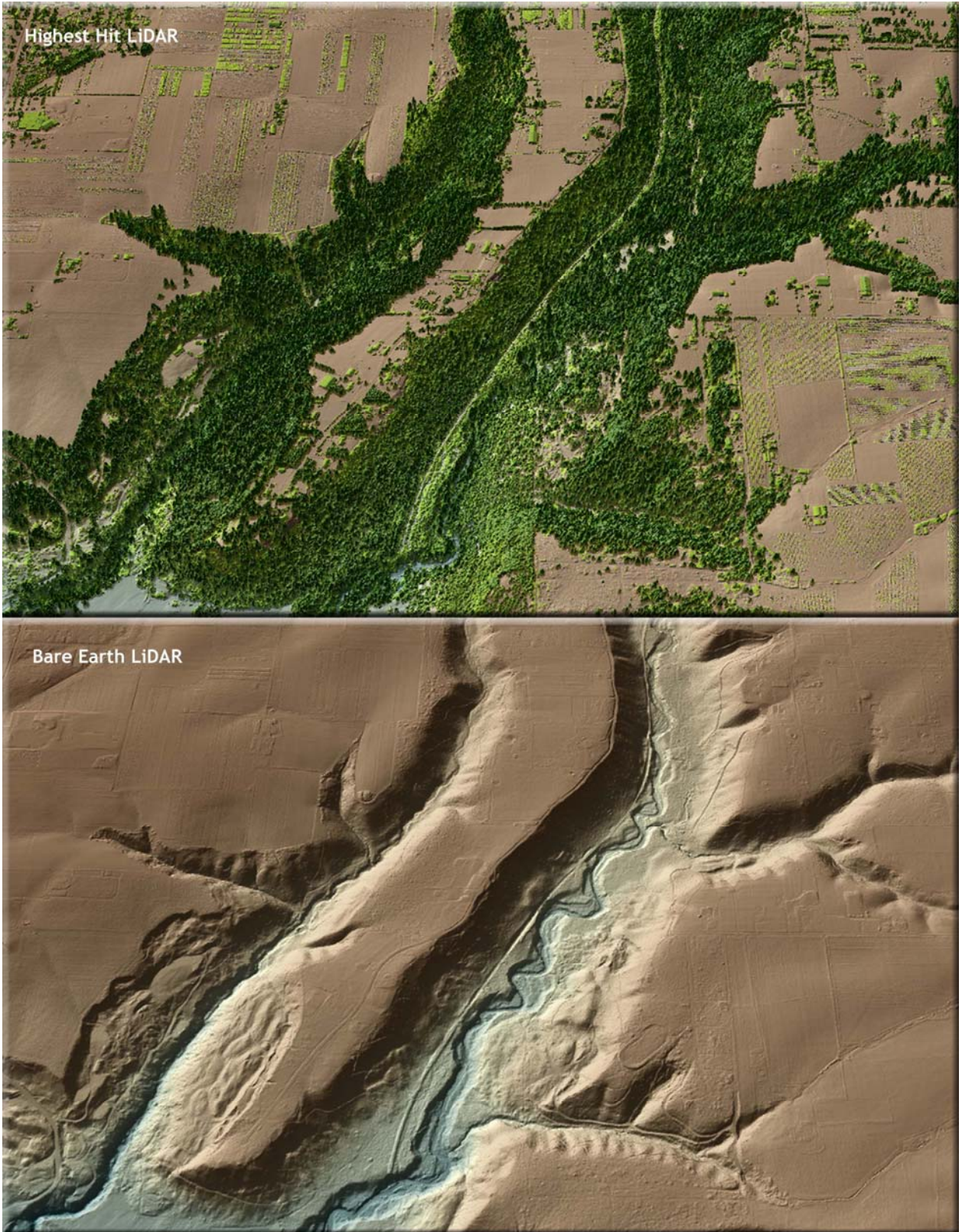
Figure 60. 3-d oblique view looking northward at the dam and powerhouse on the Clackamas River in Estacada.

Figure 61. 3-d oblique view looking northward at the confluence of Eagle Creek and North Fork Eagle Creek.

7. Glossary

1-sigma (σ) Absolute Deviation: Value for which the data are within one standard deviation (approximately 68th percentile) of a normally distributed data set.

2-sigma (σ) Absolute Deviation: Value for which the data are within two standard deviations (approximately 95th percentile) of a normally distributed data set.

Root Mean Square Error (RMSE): A statistic used to approximate the difference between real-world points and the LiDAR points. It is calculated by squaring all the values, then taking the average of the squares and taking the square root of the average.

Pulse Rate (PR): The rate at which laser pulses are emitted from the sensor; typically measured as thousands of pulses per second (kHz).

Pulse Returns: For every laser emitted, the Leica ALS 50 Phase II system can record *up to four* wave forms reflected back to the sensor. Portions of the wave form that return earliest are the highest element in multi-tiered surfaces such as vegetation. Portions of the wave form that return last are the lowest element in multi-tiered surfaces.

Accuracy: The statistical comparison between known (surveyed) points and laser points. Typically measured as the standard deviation (sigma, σ) and root mean square error (RMSE).

Intensity Values: The peak power ratio of the laser return to the emitted laser. It is a function of surface reflectivity.

Data Density: A common measure of LiDAR resolution, measured as points per square meter.

Spot Spacing: Also a measure of LiDAR resolution, measured as the average distance between laser points.

Nadir: A single point or locus of points on the surface of the earth directly below a sensor as it progresses along its flight line.

Scan Angle: The angle from nadir to the edge of the scan, measured in degrees. Laser point accuracy typically decreases as scan angles increase.

Overlap: The area shared between flight lines, typically measured in percents; 100% overlap is essential to ensure complete coverage and reduce laser shadows.

DTM / DEM: These often-interchanged terms refer to models made from laser points. The digital elevation model (DEM) refers to all surfaces, including bare ground and vegetation, while the digital terrain model (DTM) refers only to those points classified as ground.

Real-Time Kinematic (RTK) Survey: GPS surveying is conducted with a GPS base station deployed over a known monument with a radio connection to a GPS rover. Both the base station and rover receive differential GPS data and the baseline correction is solved between the two. This type of ground survey is accurate to 1.5 cm or less.

8. Citations

Soininen, A. 2004. TerraScan User's Guide. Terrasolid.